Variety is the spice of life: nongenetic variation in life histories influences population growth and evolvability

Amy B. Forsythe[1,*], Sarah P. Otto[1], William A. Nelson[2], Troy Day[2,3]

March 1, 2024

1. Department of Zoology and Biodiversity Research Centre, University of British Columbia, Vancouver, BC V6T 1Z4, Canada;

2. Department of Biology, Queen's University, Kingston, ON K7L 3N6, Canada;

3. Department of Mathematics and Statistics, Queen's University, Kingston, ON K7L 3N6, Canada.

∗ Corresponding author; e-mail: forsythe@zoology.ubc.ca.

Manuscript elements: Appendix 1, Appendix 2, Figure 1, Figure 2, Supplemental PDF (includes Figure S1, Figure S2), Supplemental *Mathematica* document.

Keywords: Individual heterogeneity, matrix population model, population dynamics, life history evolution, vital rate covariance

Abstract

Individual vital rates are key determinants of lifetime reproductive success, and variability in these rates shapes population dynamics. Previous studies have found that such heterogeneity can influence demographic parameters including population growth rates, however the explicit effects of the amount of variation within and the covariance between vital rates that can also vary throughout the lifespan on population growth remains unknown. Here, we explore the analytical consequences of nongenetic heterogeneity on long-term population growth rates and rates of evolution by modifying traditional age-structured population projection matrices to incorporate variation among individual vital rates. The model allows vital rates to be permanent throughout life ("fixed condition"), or to change over the lifespan ("dynamic condition"). We reduce the complexity associated with adding individual heterogeneity to age-structured models through a novel application of matrix collapsing ("phenotypic collapsing"), showing how to collapse in a manner that preserves the asymptotic and transient dynamics of the original matrix. The main conclusion is that nongenetic individual heterogeneity can strongly impact the long-term growth rate and rates of evolution. The magnitude and sign of this impact depends heavily on how the heterogeneity covaries across the lifespan of an organism. Our results emphasize that nongenetic variation cannot simply be viewed as random noise, but rather that it has consistent, predictable effects on fitness and evolvability.

Introduction

Just as no two snowflakes are alike, neither are two individuals. Ecologists and evolutionary biologists have long sought to capture this among individual variation in life histories because schedules of individual mortality and reproduction are key determinants of lifetime reproductive success at the individual level and fitness at the population level. Accumulating research shows that this variability among individual mortality and birth rates (collectively referred to as "vital rates") can have unexpected and major consequences for populations, including influences on population growth rates (Kendall et al. 2011; Lee et al. 2017*a*; Steiner et al. 2014), rates of evolution (Cressler et al. 2017; Jouvet et al. 2018), and viability (Acker et al. 2014; Krieger et al. 2020; Vindenes and Langangen 2015). Moreover, empirical evidence suggests that this individual heterogeneity exists in nearly all populations, from unicellular organisms to mammals (e.g., Armstrong et al. 2018; Beckage and Clark 2003; Hartemink and Caswell 2018; Jouvet et al. 2018; Rotella 2023; Tuljapurkar et al. 2009). There are countless mechanisms that may generate and maintain variability in individual vital rates, from conspicuous differences due to age (Oosthuizen et al. 2021; Tompkins and Anderson 2019), developmental stage (Bright Ross et al. 2020; Deere et al. 2017), size (Armstrong et al. 2018; Rees and Ellner 2019), sex (Broekman et al. 2020; Smallegange et al. 2018), and genotype (Cressler et al. 2017; Jouvet et al. 2018), to less obvious differences such as unequal allocation of parental care (Dudeck et al. 2018; Smiseth et al. 2007), maternal effects (Fox et al. 2006; Hernández et al. 2020; Jones et al. 2005), developmental hetergoeneity (Cooper and Kruuk 2018; Olijnyk and Nelson 2013), and environmental heterogeneity (Bruijning et al. 2019; Dahlgren et al. 2016; Douhard et al. 2013). Given the overwhelming prevalence of individual heterogeneity, studies that consider its effects on demography can provide invaluable insight about populations and their ecological and evolutionary dynamics.

A central goal across studies of individual heterogeneity is to determine how much, and when, variation among individual life histories matters for population dynamics. For example, as long as individual vital rates can persist for at least part of the life span, there is a potential

for both positive and negative covariances in survival and birth rates both across individuals and across ages, which could have complex consequences for ecological and evolutionary dynamics (Benton et al. 2006; Lee et al. 2017*a*,*b*). Indeed, negative covariances (i.e., "trade-offs") among vital rates may dampen the effects of individual heterogeneity because they minimize fitness differences among individuals. These negative covariances are consistent with traditional life-history theory that postulates a fixed energy budget for investment in survival and reproduction, such that an individual that invests heavily in one vital rate will pay a cost with a low value of another vital rate either at present or at some point in the future (Reznick 1985; Stearns 1989). On the other hand, positive covariances can structure populations into groups of high and low condition individuals, where the high condition individuals typically dominate population dynamics (Jansen et al. 2012; van de Pol et al. 2006; Zuidema et al. 2009). Here, a positive covariance implies that some "lucky" individuals are of high condition because they maintain high values of multiple vital rates and contribute disproportionately to population growth, compared to individuals in poorer condition. Positive covariances are generally expected when there is heterogeneity in resource aquisition among individuals or in resource abundance across environmental patches (Descamps et al. 2016; van de Pol et al. 2006; van Noordwijk and de Jong 1986). While some population models have suggested that covariances among vital rates across the lifespan should have little qualitative effects at the population level unless they are quite strong (González-Suárez et al. 2011; Lee et al. 2017*b*), others have found that both the magnitude and sign of the covariance between survival and birth rates can influence population dynamics (Cressler et al. 2017; Kendall et al. 2011; Stover et al. 2012). Here we use exact analytical insight to determine in general when, and how, individual heterogeneity and covariances in vital rates are expected to influence long-term population growth rates (i.e., fitness) and rates of evolution.

The presence of individual heterogeneity creates a distribution of vital rates among the individuals in a population, such that some individuals enjoy higher survival and birth rates than others (Badger et al. 2020; Cam et al. 2016, 2013; Chambert et al. 2013). The combined effects of an individual's position in each vital rate distribution determines its relative rank in a hierarchy

of overall condition (Forsythe et al. 2021; Ronget et al. 2017). Individuals with higher ranks are expected to contribute more to population growth than lower condition individuals because of their higher fitness (Coulson et al. 2006; Jansen et al. 2012; Jenouvrier et al. 2015; Zuidema et al. 2009), however these effects last only as long as an individual's relative position in the hierarchy is maintained. Accordingly, the existing literature typically classifies individual heterogeneity into two types, which are defined by whether phenotypes affecting vital rates do or do not persist across the lifespan (e.g., Bonnet and Postma 2016; Orzack et al. 2011; Tuljapurkar et al. 2009; van Daalen and Caswell 2020) and here termed "fixed condition" and "uncorrelated condition" (see Cam et al. 2016 and Forsythe et al. 2021 for reviews of terminology). This distinction is somewhat artificial in the sense that the phenotype may persist to some extent but not completely over the life span of an individual, a scenario which we call "dynamic condition" and allow below. Distinguishing individual condition by whether it is fixed or varying throughout life has proved useful for modeling the effects of individual heterogeneity on lifetime reproductive success and population growth (Orzack et al. 2011; Plard et al. 2012, 2018; Snyder and Ellner 2018).

At one extreme, fixed condition occurs when individual vital rates are set at birth and persist throughout life, such that some individuals are consistently more successful than others (Forsythe et al. 2021; Jenouvrier et al. 2022; van Daalen and Caswell 2020). For example, seeds that germinate in a particularly good micro-habitat are likely to have higher vital rates than seeds that germinate in poorer environments, and these differences would persist as long as the environmental heterogeneity is maintained. Fixed condition has been observed in probabilities of survival and breeding in the kittiwake, *Rissa tridactyla* (Cam et al. 2002, 2013; Coulson 1968; Coulson and Porter 1985) and in reproductive rates of Weddell seals, where "robust" females were expected to produce at least 1.5 times as many pups over their life as "frail" individuals (Chambert et al. 2014, 2013; Paterson et al. 2018). At the other extreme, uncorrelated condition occurs when vital rates can change randomly at any time throughout an individual's life. This type of heterogeneity is conceptually similar to what previous studies have referred to as "individual stochasticity" (e.g., Forsythe et al. 2021; van Daalen and Caswell 2020), "luck" (e.g., Snyder and

Ellner 2018, 2022), or "dynamic heterogeneity" (e.g., Steiner et al. 2010; Tuljapurkar et al. 2009), however an important distinction is that here we use "uncorrelated condition" to refer to random variation among individual vital rates, not individual fates. In between these two extremes, dynamic condition allows vital rates to vary throughout the life course, but relaxes the assumption of random transitions by allowing some dependency of future vital rates on an individual's current age or phenotype. Compared to fixed condition, where an individual's future vital rates are exactly determined by its current vital rates, dynamic condition allows these vital rates, and therefore an individual's expected fitness, to vary over the life course. For example, heavier animals tend to have higher vital rates (e.g., Bonnet et al. 2017; Clutton-Brock et al. 1987; Hamel et al. 2009; Nussey et al. 2011), however an individual's body mass may increase or decrease from year to year. Individual survival probabilities can also vary with environmental conditions in a given year (e.g., in the Raso lark, *Alauda razae* (Dierickx et al. 2019)), and there is evidence that reproductive rates change with age across many species, including red deer, *Cervus elaphus* (Moyes et al. 2011), grey seals, *Halichoerus grypus* (Badger et al. 2020), spotted turtles, *Clemmys guttata* (Feng et al. 2019), and Nazca boobies, *Sula granti* (Tompkins and Anderson 2019).

Previous theoretical studies have revealed that individual heterogeneity in vital rates can influence key demographic parameters, from extinction risks and viability (Acker et al. 2014; Fox 2005; Knight et al. 2008; Vattiato et al. 2021; Vindenes et al. 2008, 2012) to generation times and net reproductive rates (Bliard et al. 2024; Steiner et al. 2014; Vindenes and Langangen 2015). Among these, Kendall et al. (2011) developed a population model with overlapping generations allowing two categories of individuals (high and low fixed condition in either survival probabilities or fecundities), but without age or stage structure in vital rates; heterogeneity in survival probabilities had a "previously unrecognized effect," increasing the asymptotic population growth rate via "cohort selection," whereby the higher condition individuals out-survived those in lower condition. Building on this work, Stover et al. (2012) incorporated fixed condition by setting mortality rates, birth rates, or both to a high or low value in a density-dependent logistic model and found that the low-density growth rate depends on the strength of individual heterogeneity as well as

the correlation among vital rates. These models suggest that heterogeneity in vital rates can have a strong influence on population growth rates when these rates remain constant as an individual ages, however we still lack theory for the influence of such heterogeneity on population growth rates when vital rates can vary with age. While integral projection models (IPMs) have provided theoretical insight to the effects of individual heterogeneity that can change with age on lifetime reproductive success (Snyder and Ellner 2018; Snyder et al. 2021), to our knowledge analyses of population growth using IPMs have remained numerical thus far (e.g., Fung et al. 2022; Kentie et al. 2020; Plard et al. 2016, 2018; Vindenes and Langangen 2015). This is in part because including heterogeneous vital rates in age-structured populations allows for much more complexity, as the condition of an individual can change over their life span, with the potential for both positive and negative covariances in age-specific survival and fertility rates.

There is a large body of work that has incorporated vital rate variation in age- and stage-structured models to calculate lifetime reproductive success and the relative contributions of fixed heterogeneity classes versus individual stochastic differences to this fitness component (e.g., Hernández-Pacheco and Steiner 2017; Jenouvrier et al. 2015; Plard et al. 2012; Snyder and Ellner 2018, 2022; Snyder et al. 2021; Tuljapurkar et al. 2009, 2020; van Daalen and Caswell 2020). Several studies have used these analyses of lifetime reproductive success along with generation time to estimate how among-individual variation may also influence population growth rates (e.g., Steiner and Tuljapurkar 2012; Steiner et al. 2014). This question has also been investigated through numerical approaches (Knight et al. 2008; Plard et al. 2018), however the explicit effects of the amount of variation within and the covariance among survival and birth rates on population growth and fitness are still unknown. Furthermore, in evolutionary studies these stochastic differences in age-specific vital rates are generally considered neutral with respect to selection while the fixed differences are considered to be genetically based and adaptive; under this assumption, stochastic variation in vital rates throughout the life course can magnify the effect of random drift in populations and slow the rate of evolutionary change compared to what is expected from fixed genetic differences alone (Coste and Pavard 2020; Steiner and Tuljapurkar

2012; van Daalen and Caswell 2020). A much less explored question is how *nongenetic* heterogeneity that persists over the lifespan could influence ecological and evolutionary dynamics. In this study we develop a conceptual unification of the influences of nongenetic heterogeneity on population growth rates and rates of evolution, with a particular emphasis on the impact of the covariance among vital rates throughout the lifespan.

Traditional evolutionary studies often focus on genetic variation that is heritable and so can generate evolutionary change (Huxley 1942; Mayr 1982). Yet, nongenetic factors can be just as, if not more, important than genetics in determining an individual's fitness (Cressler et al. 2017; Gomes et al. 2019; Jouvet et al. 2018; Olijnyk and Nelson 2013) and there is accumulating evidence for nongenetic inheritance (Bonduriansky and Day 2009, 2018; Day and Bonduriansky 2011). Moreover, these effects of nongenetic variation can scale up to influence ecological and evolutionary dynamics. For example, Jouvet et al. (2018) identified variation in lifespan and lifetime reproduction in clonal cells of the bacteria *Escherichia coli*, which shifted the clonal population growth rate (fitness) away from what would be predicted if all cells had followed the same life-history schedule represented by the mean lifespan and mean lifetime reproduction of the clone. Nongenetic individual heterogeneity could also play a dominant role for determining evolutionary dynamics in *Daphnia pulicaria*, where it has been observed that even in the same environment, there is more variation in mortality, birth, and development rates among individuals within a clonal genotype than there is among genotypes (Cressler et al. 2017; Olijnyk and Nelson 2013). An individual-based simulation incorporating these genetic and nongenetic sources of individual heterogeneity found that increasing the relative strength of nongenetic heterogeneity can influence population growth rates and slow rates of evolution by natural selection (Cressler et al. 2017). The effects depended on the sign of the nongenetic and genetic covariances among vital rates, however the general mathematical relationships between these covariances and rates of evolution and population growth are still unknown.

Here, we explore the consequences of different types of nongenetic individual heterogeneity on the long-term growth rate (fitness) of a genotype, allowing us to determine the impact of this

heterogeneity on the rate of evolution by natural selection. We modify traditional age-structured population projection matrices (Leslie matrices) to incorporate individual heterogeneity among survival probabilities and birth rates. We assume that each population projection matrix represents a single, clonal genotype, such that all individual heterogeneity within a matrix is attributed to nongenetic sources. The model includes further biological realism by allowing arbitrary transitions in phenotype over the lifespan, however in order to gain analytical insight we assume that the heterogeneity is reset among the offspring in each generation (an assumption that could be relaxed in future numerical analyses). This assumption allows us to introduce "phenotypic collapsing" as a method to reduce the complexity associated with adding individual heterogeneity to age-structured models, while preserving both the transient and asymptotic dynamics of the original system. Genetic variation is incorporated by considering multiple clonal genotypes, each with their own transition matrix with nongenetic heterogeneity. We compare the long-term growth rate and evolvability across a broad range of genetic and nongenetic covariances and across different strengths of nongenetic variation. The main conclusion is that nongenetic individual heterogeneity strongly impacts the long-term growth rate and rates of evolution by natural selection in the model. The magnitude and even the sign of this impact depends on whether the heterogeneity is fixed or varying across the lifespan and on how the heterogeneity co-varies across vital rates experienced over the life course. Our results emphasize that nongenetic variation cannot simply be viewed as random noise because it has predictable effects on fitness and evolvability.

Methods and Results

We modify classic age-structured population projection matrices to study the evolutionary consequences of nongenetic individual heterogeneity. Our approach begins by considering the fitness of a single genotype with vital rates that are assigned at birth and either permanent throughout life (fixed condition) or allowed to change throughout the life course (dynamic condition). Vital

rates that vary over the lifespan may depend on the individual's current age and phenotype, or may be be drawn randomly at each age (uncorrelated condition). We then use this analysis to understand how nongenetic heterogeneity in condition influences the long-term growth rate and rate of evolution by natural selection across multiple genotypes in a population.

Analysis - Single Genotype

The traditional form of an age-structured population projection matrix assumes that individuals can be classified into states that depend only on their age (Leslie 1945). The full population projection matrix model is needed to predict short-term ("transient") dynamics, while the long-term ("asymptotic") dynamics are determined knowing only the leading eigenvalue (λ_1, which gives the asymptotic population growth rate) and its corresponding right and left eigenvectors (which give the stable-age distribution and age-specific reproductive values, respectively) (Caswell 2001). Here we assume that each transition matrix describes an isolated population consisting of a single genotype, and consider λ_1 to be the relevant measure of genotype fitness. Scaling up to a population of multiple genotypes, the variance among the single-genotype growth rates predicts the rate of fitness increase under the assumption of no interaction or mating among genotypes (Fisher 1930).

To explore the fitness consequences of different types of nongenetic individual heterogeneity, we allow both vital rates in the Leslie matrix (survival probabilities, s, and birth rates, b) to vary among individuals within each age class. Individuals are assigned a value for each vital rate at birth, and these rates are either permanent (fixed condition) or can vary arbitrarily throughout life (dynamic condition).

We first develop a simple example for a single genotype with two age classes and two potential values of each vital rate to highlight the structural differences between life histories that are fixed or varying across life and to investigate how these differences influence genotype fitness. We then extend this model to an arbitrary number of age classes and values of each vital rate and describe how the resulting large-scale matrices can be collapsed to matrices with a single set of

effective vital rates for each age class, while still providing the complete solution to the original model. Note that this means that the eigenvalues and eigenvectors of the reduced system completely characterize the solution of the original full system (after a maximum of one generation, see Appendix 1). Throughout, we assume that population sizes are large, and so we can ignore stochastic variation in the realized heterogeneity that would be expected in smaller populations (e.g., Gillespie 1973, 1974, 1977). Finally, we conduct a numerical analysis to explore the relative importance of genetic and nongenetic sources of heterogeneity to the mean long-term growth rate and rate of evolution in a population of different genotypes.

A Simple Example

Consider an age-structured clonal population of a single genotype with no density-dependence and two age classes: non-reproductive juveniles (J) and reproductive adults (A). The Leslie matrix is

$$\mathbf{L} = \begin{bmatrix} 0 & b \\ s & 0 \end{bmatrix} \tag{1}$$

This matrix assumes that the survival rate of juveniles to adults (s) and the birth rate of adults (b) is the same for all individuals and that all adults die after giving birth.

To incorporate individual heterogeneity in this model, assume that individuals can express one of ρ different phenotypes, each with their own unique potential vital rates. Here we use the term "phenotype" to distinguish variants that are produced by nongenetic variation from those that are produced by genetic variation, however the vital rates do not need to be directly observable. Individuals of phenotype x survive with probability s_x and give birth to b_x offspring over a single time step.

For this simple example with two age classes, we consider two phenotypes in the population. The first phenotype is represented by a set of vital rates (s_1, b_1) and the second phenotype by a separate set of vital rates (s_2, b_2). At a given time, individuals can belong to one of four possible

states in this model, such that

$$\vec{N}(t) = \begin{bmatrix} J_1, & J_2, & A_1, & A_2 \end{bmatrix}^T \tag{2}$$

where $\vec{N}(t)$ is the state vector at time t, and J_x and A_x represent the number of juveniles and adults of phenotype x at time t, respectively. A core assumption that we make is that the phenotypic heterogeneity we are tracking is not heritable, so that adults give birth to offspring of phenotype x with probability given by j_x, regardless of the parental phenotype. Further, we let $j_1 + j_2 = 1$, so that all offspring must be born into one of the two phenotypes and there is no death of newborns from the transition process.

Under fixed condition, an individual's vital rates are fixed for life. Thus, individuals may be born from a parent of either phenotype, but once the phenotype is assigned it determines an individual's survival probability and birth rate for its entire life. The transition matrix for a genotype with fixed condition is therefore

$$\mathbf{L_F} = \begin{bmatrix} 0 & 0 & j_1 b_1 & j_1 b_2 \\ 0 & 0 & j_2 b_1 & j_2 b_2 \\ s_1 & 0 & 0 & 0 \\ 0 & s_2 & 0 & 0 \end{bmatrix} \tag{3}$$

where the rows and columns of the transition matrix follow the same phenotype and age structure as the state vector $\vec{N}(t)$ (equation (2)).

In contrast, the dynamic condition model allows individuals to transition between phenotypes throughout their life. At each time step, we assume that an individual transitions from phenotype x to phenotype y with probability $f_{x \to y}$. For example $f_{2 \to 1} s_2$ would represent the fraction of juveniles born in phenotype 2 that survive (with probability s_2) and transition to phenotype 1 as adults (and then have birth rate b_1). In the case of only two age classes there is only one possible age transition for surviving individuals (age 1 to 2), however in the next section we allow this transition probability to also depend on an individual's age. The transition matrix for

a genotype with vital rates that can vary throughout life is therefore

$$\mathbf{L_D} = \begin{bmatrix} 0 & 0 & j_1 b_1 & j_1 b_2 \\ 0 & 0 & j_2 b_1 & j_2 b_2 \\ f_{1\to1} s_1 & f_{2\to1} s_2 & 0 & 0 \\ f_{1\to2} s_1 & f_{2\to2} s_2 & 0 & 0 \end{bmatrix} \tag{4}$$

This model reduces to uncorrelated condition, where phenotypes are randomly determined at each age, when $f_{x\to y} = f_{y\to y} = f_y$ for all phenotypes x and y (i.e., the probability of transitioning into a given phenotype is the same for all individuals of a given age).

Consider the long-term growth rates of the fixed and dynamic matrices in equations (3) and (4). Both of these are given by the leading eigenvalue of the transition matrices above

$$\begin{aligned} \lambda_1 &= \sqrt{E[sb]} \\ &= \sqrt{E[s]E[b] + Cov(s,b)} \end{aligned} \tag{5}$$

Here, $E[sb]$ can be thought of as the expected value of the adult birth rate, accounting for all of the possible life history "paths" (phenotypic transitions and corresponding survival probabilities) that allow an individual to survive to the adult class in one of the two phenotypes. Writing this quantity in terms of the covariance among vital rates requires separating these expectations, where $E[s]$ gives the expected survival probability to the adult age class, while $E[b]$ gives the expected birth rate, now independent of survival but still taken over all of the possible phenotypic transitions that an individual could have experienced throughout its life course. In the case of dynamic condition, for example, there are two ways for individuals to survive and give birth in each phenotype y: they can either be born in that phenotype and stay there, or they can be born in the second phenotype but transition to phenotype y as they age from the juvenile to the adult class, such that

$$\begin{aligned} E[sb] &= \left(j_1 s_1 + j_2 s_2\right)\left(f_1 b_1 + f_2 b_2\right) + Cov(s,b) \\ &= j_1 s_1 f_{1\to1} b_1 + j_1 s_1 f_{1\to2} b_2 + j_2 s_2 f_{2\to1} b_1 + j_2 s_2 f_{2\to2} b_2 \end{aligned} \tag{6}$$

where f_y represents all of the possible phenotypic transitions that an individual could have experienced to belong to phenotype y as an adult. For this example, $f_1 = j_1 f_{1\to1} + j_2 f_{2\to1}$ and $f_2 = j_1 f_{1\to2} + j_2 f_{2\to2}$. By contrast, with fixed condition, juveniles must survive and give birth in the phenotype that they are born with, such that

$$\begin{aligned} E[sb] &= \left(j_1 s_1 + j_2 s_2\right)\left(f_1 b_1 + f_2 b_2\right) + Cov(s, b) \\ &= j_1 s_1 b_1 + j_2 s_2 b_2 \end{aligned} \tag{7}$$

where now $f_1 = j_1$ (because $f_{1\to1} = 1$ and $f_{1\to2} = 0$ by definition of fixed condition) and correspondingly $f_2 = j_2$.

Importantly, equation (5) reveals that a genotype's fitness will be different from what would be expected with independent vital rates any time that there is a nongenetic covariance among survival to the adult class and the birth rate within that class. The only case where this covariance will be 0 is when the vital rates are stochastic throughout the lifespan, such that individuals transition randomly to any phenotype at any time (uncorrelated condition with $f_{1\to1} = f_{2\to1}$ and $f_{1\to2} = f_{2\to2}$). Correspondingly, the covariance will be strongest when vital rates are fixed throughout the lifespan. Thus, given the same age structure, individual vital rates, and transition probabilities, a genotype's fitness will be greater than expected with uncorrelated vital rates when survival probabilities and birth rates are positively related and lower than its fitness with uncorrelated condition when survival probabilities and birth rates are negatively related.

The relationship between the type of individual heterogeneity, the type of covariance, and the population growth rate can be explained by the fraction of individuals that have the greatest survival probability as juveniles and the greatest birth rate as adults. These high condition individuals contribute disproportionately to a genotype's fitness, through their own survival and through their offspring. For example, without loss of generality, assume that phenotype 1 individuals have the highest survival probability and the highest birth rate in a genotype with a positive covariance among vital rates. Comparing the two extremes at the stable phenotype distribution (defined below), the proportion of individuals in this class with fixed condition is $\frac{j_1 s_1}{E[s]}$ and with uncorrelated condition is $\frac{j_1 s_1 f_1}{E[s]}$. Assuming there is heterogeneity ($0 < f_1 <$

1), the fraction of high condition individuals will always be greater with fixed condition than with uncorrelated condition, explaining why population growth rates are higher under fixed condition when vital rates positively covary. Analogous calculations show that if there is a trade-off between survival probabilities and birth rates ($Cov(s, b) < 0$), the proportion of high condition individuals (for example, phenotype 1 for survival but phenotype 2 for reproduction) will always be greater with uncorrelated condition than with fixed condition (Supplemental material S1).

The influence of the covariance among vital rates on population dynamics is underscored by considering an example population where juveniles keep their phenotype to the adult age class with probability τ (fixed condiiton), and correspondingly, are assigned a random phenotype with probability $1 - \tau$ (uncorrelated condition). The long-term population growth rate is then

$$\lambda_1 = \sqrt{(1-\tau)\, E[s]E[b] + \tau E[sb]} \tag{8}$$

The sensitivity of the long-term population growth rate with respect to τ is

$$\frac{\partial \lambda_1}{\partial \tau} = Cov(s, b) \tag{9}$$

Accordingly, when the covariance among survival probabilities and birth rates is positive, an increase in the persistence of vital rates throughout an individual's life course (τ) will increase the population growth rate; negative covariances have the opposite effect.

The Full Model

We now consider ρ vital rate phenotypes and ω ages. This general model allows reproduction from individuals of any age and it allows individuals to survive up to age ω. At a given time, an individual belongs to one of $\rho \cdot \omega$ states. Thus, the state vector is

$$\vec{N}(t) = \left[n_{1,1}, \cdots n_{\rho,1}, n_{1,2}, \cdots n_{\rho,2}, \cdots n_{1,\omega}, \cdots n_{\rho,\omega} \right]^T \tag{10}$$

Further, let

$$\mathbf{B}_{\boldsymbol{\rho},\boldsymbol{a}} = \begin{bmatrix} j_1 b_{1,a} & j_1 b_{2,a} & \cdots & j_1 b_{\rho,a} \\ j_2 b_{1,a} & j_2 b_{2,a} & \cdots & j_2 b_{\rho,a} \\ \vdots & \vdots & \vdots & \vdots \\ j_\rho b_{1,a} & j_\rho b_{2,a} & \cdots & j_\rho b_{\rho,a} \end{bmatrix} \tag{11}$$

be a matrix of the potential birth rates from individuals of age a to any of the ρ phenotypes, where j_x represents the probability that an adult of age a gives birth to offspring that are in phenotype x at age 1. Assume that

$$\sum_{x=1}^{\rho} j_x = 1 \tag{12}$$

so that all offspring from individuals of age a must be born into one of the ρ phenotypes and there is no death of newborns from the transition process. These transition probabilities do not depend on the phenotype or age class of the parent, a limiting assumption that we make in order to collapse the matrices without loss of information about the dynamics as described later in this section. Note, however, that there will often be some kind of parent-offspring correlation (e.g., due to maternal effects, nongenetic inheritance, or correlated environments between parents and offspring (Bonduriansky and Day 2009; Danchin et al. 2011; Hernández et al. 2020)), which must be treated using the full phenotype-age matrix to preserve the full population dynamics and eigenstructure (although the leading eigenvalue and stable age distribution can still be obtained by collapsing the matrix as described below, see Hooley 2000 and Coste et al. 2017).

To incorporate heterogeneity throughout the lifespan, suppose that the potential survival and transition probabilities for individuals of age a and phenotype x are given by the matrix

$$\mathbf{S}_{\boldsymbol{\rho},\boldsymbol{a}} = \begin{bmatrix} f_{1\to1,a} s_{1,a} & f_{2\to1,a} s_{2,a} & \cdots & f_{\rho\to1,a} s_{\rho,a} \\ f_{1\to2,a} s_{1,a} & f_{2\to2,a} s_{2,a} & \cdots & f_{\rho\to2,a} s_{\rho,a} \\ \vdots & \vdots & \vdots & \vdots \\ f_{1\to\rho,a} s_{1,a} & f_{2\to\rho,a} s_{2,a} & \cdots & f_{\rho\to\rho,a} s_{\rho,a} \end{bmatrix} \tag{13}$$

Here, $f_{x\to y,a}$ represents the probability that a surviving individual of phenotype x at age a transitions into phenotype y by age $a+1$. These transition probabilities can depend on an individual's

current and future age and phenotype. For notational simplicity, we include only the subscript for the current age in these transition probabilities, since the next age is directly determined by the current age a (individuals cannot skip or move backwards in age). Further, assume that

$$\sum_{y=1}^{\rho} f_{x \to y,a} = 1 \tag{14}$$

and so there is no loss of surviving individuals due to the transition process for any age a or phenotype x. This matrix allows transitions between phenotypic classes at arbitrary rates, including the two extreme types of individual heterogeneity (fixed and uncorrelated condition). If $f_{x \to y,a} = 1$ when $x = y$ and is 0 otherwise, then the phenotypes are permanent throughout life (fixed condition), while if $f_{x \to y,a} = f_{y \to y,a} = f_{y,a}$ for all phenotypes x and y then the condition is uncorrelated, with phenotypes randomly drawn at each age. An intermediate choice allows the phenotype to be correlated from one age to the next, with probability τ of remaining in the same phenotype and probability $(1 - \tau) f_{y,a}$ of being assigned a phenotype at random in the next time step (here τ measures the strength of the phenotypic correlation between age classes).

Under these assumptions, the ρ-phenotype ω-age transition matrix takes the form

$$\mathbf{L}_{\rho,\omega} = \begin{bmatrix} \mathbf{B}_{\rho,1} & \mathbf{B}_{\rho,2} & \mathbf{B}_{\rho,3} & \cdots & \mathbf{B}_{\rho,\omega-1} & \mathbf{B}_{\rho,\omega} \\ \mathbf{S}_{\rho,1} & 0 & 0 & \cdots & 0 & 0 \\ 0 & \mathbf{S}_{\rho,2} & 0 & \cdots & 0 & 0 \\ 0 & 0 & \mathbf{S}_{\rho,3} & \cdots & 0 & 0 \\ \vdots & \vdots & \vdots & \ddots & \vdots & \vdots \\ 0 & 0 & 0 & \cdots & \mathbf{S}_{\rho,\omega-1} & 0 \end{bmatrix} \tag{15}$$

where $\mathbf{L}_{\rho,\omega}$ is a square matrix of size $\rho \cdot \omega$-by-$\rho \cdot \omega$ and each 0 in $\mathbf{L}_{\rho,\omega}$ is a $\rho \cdot \rho$ block of 0's. Readers familiar with IPMs will recognize this structure (Easterling et al. 2000; Ellner and Rees 2006) and could easily extend our model to compare the effects of different kinds of heterogeneity when phenotypic classes are continuous.

The generalized transition matrix in equation (15) can be used to predict ecological and evolutionary dynamics more accurately than matrices that oversimplify the true number of pheno-

types and age classes in a population. However, the matrices will often be very large if they account for the number of phenotypes and age classes found in real populations. For example, if there are only five potential phenotypes for survival, five for birth rates, and two age classes in a population, the matrix accounting for individual heterogeneity will already be of size $(5 \cdot 5 \cdot 2) \times (5 \cdot 5 \cdot 2) = 50 \times 50$.

Here we present a novel matrix collapsing method to reduce the ρ-phenotype ω-age matrix to an ω-age matrix that contains a single phenotype for each age class. Accordingly, these collapsed matrices take the same form as traditional Leslie matrices. This technique was inspired from previous work that shows how to collapse population projection matrices across age or stage classes (Enright et al. 1995; Hooley 2000; Salguero-Gómez and Plotkin 2010). Although these previous matrix collapsing methods typically only guarantee that the long-term growth rate and stable age distribution of the original matrix are captured by the collapsed matrix (Coste et al. 2017; Hooley 2000; with the method of Bienvenu et al. 2017 also preserving reproductive values), we prove that the full solution of the original matrix model is captured by our method for the kinds of matrices considered here, where phenotypes among newborns are chosen at random (Appendix 1; see examples in Supplemental material S2). This means that the collapsed matrix captures both the transient and asymptotic dynamics of age-structured populations with such nongenetic heterogeneity in vital rates, after a short transition period of at most ω time steps (see Supplemental material 2 for an example) and that all eigenvalue and eigenvector pairs of the collapsed system completely characterize the solution of the full system (see Appendices).

Briefly, our application of matrix collapsing (termed "phenotypic collapsing") merges the rows and columns corresponding to the ρ phenotypes within each age class (see Appendix 1 for the full recipe). The phenotypes are weighted by the proportion of individuals in age a and phenotype x, that are expected from offspring born a time steps ago, considering all phenotypic transitions and survival rates that could have occurred in between ($\psi_{x,a}$, see Appendix 1; Appendix 2). This expectation is the same regardless of the eigenvalues of the full matrix and after ω time steps gives the stable phenotypic distribution for that age class. A major advantage of phe-

notypic collapsing is that it does not require that the system is at a stable age distribution, which is different from classic matrix collapsing that uses the stable age distribution to determine the collapsing weights (Enright et al. 1995; Hooley 2000). Additionally, phenotypic collapsing does not rely on calculating and weighting by the eigenvectors, requiring only the total probability of all possible paths from birth to survival at age a with phenotype x (a total that is described by a simple matrix power, see Appendix 1). A full worked example of collapsing a transition matrix with two phenotypes and two or three age classes to a transition matrix with a single-phenotype for each age class is found in Supplemental material S2.

Define l_a as the probability of surviving up to age a. The collapsed ω-age matrix can then be shown to equal

$$\mathbf{L}_{\boldsymbol{\omega}} = \begin{bmatrix} E[b_1] & \frac{Cov(l_2, b_2)}{E[l_2]} + E[b_2] & \frac{Cov(l_3, b_3)}{E[l_3]} + E[b_3] & \cdots & \frac{Cov(l_{\omega-1}, b_{\omega-1})}{E[l_{\omega-1}]} + E[b_{\omega-1}] & \frac{Cov(l_\omega, b_\omega)}{E[l_\omega]} + E[b_\omega] \\ E[s_1] & 0 & 0 & \cdots & 0 & 0 \\ 0 & \frac{Cov(l_2, s_2)}{E[l_2]} + E[s_2] & 0 & \cdots & 0 & 0 \\ 0 & 0 & \frac{Cov(l_3, s_3)}{E[l_3]} + E[s_3] & \cdots & 0 & 0 \\ \vdots & \vdots & \vdots & \ddots & \vdots & \vdots \\ 0 & 0 & 0 & \cdots & \frac{Cov(l_{\omega-1}, s_{\omega-1})}{E[l_{\omega-1}]} + E[s_{\omega-1}] & 0 \end{bmatrix} \tag{16}$$

where the matrix entries are calculated using the phenotypic collapsing recipe provided in Appendix 1. The covariances (Cov) are taken between all of the possible phenotypic histories that an individual could have experienced to survive up to a given age a (l_a), and the birth rate (top row) or survival probability (subdiagonal) at that age. The expectations of the vital rates at age a, $E[s_a]$ and $E[b_a]$, are taken over all of the possible phenotypic transitions that an individual could have experienced up to age a, independent of survival along the way (i.e., with $\psi_{x,a} = f_{x,a}$ for each phenotype x at age $a > 1$ and j_x for the newborns, see Appendices for proof and Supplemental material S2 for examples). These are the expected values of the vital rates that would be obtained if the current phenotype did not depend on any previous phenotype (uncorrelated condition), and so can be calculated as an average taken only over the phenotypic distribution

at that age. The expectation $E[l_a]$ is the expected probability of surviving to age a, considering all of the possible phenotypes and corresponding survival probabilities that an individual could have experienced throughout its life course from age 1 to a (i.e., with $\psi_{x,a}$ depending on previous transition and survival probabilities, see Appendices and examples in Supplemental material S2).

The collapsed matrix $\mathbf{L}_\omega$ reveals that when the current survival and birth rates are independent of the life history path that an individual took to get there (i.e., the heterogeneity is uncorrelated and phenotypes are randomly determined at each age), all covariances are 0 and the effective vital rates can be calculated as a weighted average considering only the vital rates and transition probabilities assigned to each age (ignoring any previous transition or survival probabilities, such that $\psi_{x,a} = f_{x,a}$ or j_x as mentioned above). All else being equal, increasing the covariance between survivorship to age a and the survival probability or birth rate at age a will increase the effective vital rates in equation (16). Consequently, when there is a positive covariance among vital rates over the lifespan, the long-term growth rate will be higher than predicted using only the average vital rates at each age, with the opposite holding when there are trade-offs among vital rates.

Another important observation is that the collapsed vital rates in equation (16) are simply the average vital rates of individuals surviving to age a (Appendix 2). Considering the collapsed matrix in this way underscores its value for providing straightforward predictions of ecological and evolutionary dynamics even when there are many heterogeneity classes in a population, however it overlooks the influence of the covariance among vital rates on these dynamics (see Discussion below).

The collapsed matrix can be used to analyze populations with vital rate heterogeneity, without requiring extra matrix dimensions to account for this individual variation. Indeed, when applied to matrices in the form of equation (16), we find that phenotypic collapsing preserves the complete solution of the original matrix for all times $t \geq \omega$, such that the eigenvalue and eigenvector pairs of the collapsed system completely characterize the full system (Appendix 1; see examples in Supplemental material S2). We have also found that all non-zero eigenvalues

and their associated eigenvectors from the original ρ-phenotype ω-age matrix are captured by the collapsed matrix, as long as the population has reached a stable phenotype distribution (this is proven for cases with non-repeating eigenvalues in Supplementary material S2 and will be proved more generally in a forthcoming article). This property holds because the weights that are used to collapse do not depend on the chosen eigenvalue or eigenvector once the distribution of phenotypes is constant from one generation to the next. In our case, this condition is satisfied because there is no inheritance of phenotypes from parents to offspring, and so the stable phenotype distribution is achieved within a singe generation as the distribution of phenotypes at birth is fixed and independent of the population vector. Thus, while matrix collapsing using the right eigenvector (here, the stable age *and* phenotype distribution) was already known to preserve the asymptotic population growth rate (λ_1) and its associated right eigenvector (stable age distribution) (Hooley 2000) and in some cases can also maintain the associated left eigenvector (reproductive values) (Coste et al. 2017) of the original full size matrix, here we show that phenotypic collapsing also preserves the full solution and so the transients as well for some kinds of matrices (e.g., when the heterogeneity is "reset" at some age, as in equation (15)).

Simulations - Multiple Genotypes

To explore the ecological and evolutionary consequences of nongenetic heterogeneity in vital rates when multiple clonal genotypes are co-evolving, we compliment our single-genotype analyses with randomly simulated genotypes and calculate the mean long-term growth rate and evolvability (rate of evolution by natural selection) among them. For simplicity, this numerical analysis considers only the two extreme types of nongenetic individual heterogeneity: fixed and uncorrelated condition. By definition the mean long-term growth rate is the mean fitness for a genotype, however in many empirical studies mean fitness is approximated by the average number of surviving offspring per parent. For clarity, we use the term "long-term growth rate" here. Relative evolvability is calculated as the response to selection, standardized by the mean long-term growth rate (i.e., evolvability = $var(\lambda)/\overline{\lambda}^2$) (Houle 1992). Specifically, $var(\lambda)/\overline{\lambda}$ is

the expected change in the long-term growth rate per unit time, while $var(\lambda)/\overline{\lambda}^2$ provides the expected proportional change. This approach standardizes the variance in genotype growth rates and thus allows comparison across different strengths and types of nongenetic (co)variance. Note that relative evolvability is influenced both by the mean and variance in long-term growth rates; hence we provide results for the unstandardized variance in Supplemental material S4 (fig. S1; fig. S2). We use a small number of age classes and vital rate phenotypes to facilitate comparison with the single-genotype analysis, however the model is easily extended to incorporate more complex population structures.

Recalling that the sign of the covariance among individual vital rates can influence genotype fitness, we consider positive, zero, and negative genetic and nongenetic covariances among survival probabilities and birth rates. We scale the relative amount of nongenetic variation from 0 to 5 times the amount of genetic variation, which is held constant throughout all simulations. The general modeling procedure is described below and full details can be found in the Supplemental material S3. All simulations were performed in the R statistical environment (ver. 4.3.1; R Core Team 2023). The full R code is provided in Forsythe et al. (2024) (`https://datadryad.org/stash/share/8Yh2oLMu4BXHhrurxgKfd1DEZjM2BqvteGyeyCQ4tz8`).

A genotype is defined by its set of mean vital rates. To ensure constant and biologically realistic genotype means (i.e., all survival probabilities between 0 and 1 and all birth rates greater than or equal to 0), we randomly drew vital rates from a bivariate uniform distribution. The genetic covariance was incorporated with a positive, negative, or 0 covariance in the variance-covariance matrix.

To keep the simulations at least somewhat tractable and compatible with our analytical results, we assume that each genotype contains only two possible phenotypes for each vital rate. The strength of the nongenetic variance determines how far the individual survival probabilities and birth rates fall above (phenotype 1) or below (phenotype 2) their genotypic mean. We allow the strength of the nongenetic variance to range from 0 to 5 times as much as the genetic variance, which is held constant throughout all simulations. Note that because the phenotypic means are

held constant (at the genotypic mean), the only variable that changes across our simulations is the strength of the nongenetic heterogeneity.

The final step to parameterize the single-genotype matrices is to calculate the transition probabilities for each phenotype. For simplicity we assume that the transition probabilites are independent of age and either completely determined by previous vital rates (fixed condition) or independent of any previous vital rates (uncorrelated condition), however this assumption could be relaxed, allowing partial persistence of the phenotype from age-to-age as in equation (13). The transition probabilities are calculated as the fraction in each quadrat under a bivariate normal distribution that is centered at the genotypic mean vital rates and with nongenetic covariance given by one of the three structures defined earlier: zero, positive, or negative.

Given the individual vital rates and the transition probabilities, we can parameterize the fixed and uncorrelated condition matrices for a population with any number of non-reproductive and reproductive ages. Here, we consider mean fitness and evolvability for a population with one juvenile age and one adult age (early recruitment into the breeding population) and for a population with ten juvenile ages and one adult age (late recruitment). The early recruitment example matches the simple example in the theoretical analysis, but with a total of four phenotypes to account for all possible combinations of two survival probabilities and two birth rates. To facilitate comparison, we use the same vital rates, transition probabilities, and number of juvenile and adult ages to parameterize the fixed and uncorrelated condition matrices.

First consider the results with early recruitment (fig. 1). Recall from equation (16) that the fitness of a genotype with uncorrelated condition depends only on the expected values of the age-specific survival probabilities and birth rates at the age they are experienced, while the fitness of a genotype with fixed condition depends on these expected values *and* the nongenetic covariance among these vital rates and all of the possible ways that an individual could have survived to experience them. All else being equal, positive nongenetic covariances increase the average vital rates in the transition matrix with fixed condition, and this is expected to translate into an increase in the population growth rate, while negative covariances have the opposite effect. These results

scale up to determine the mean long-term growth rate among genotypes, which for uncorrelated condition is constant regardless of the nongenetic covariance because the expected values of the vital rates are held constant in all simulations (fig. 1A). The results for fixed condition are also exactly predicted from the theoretical analyses, where a stronger positive covariance among vital rates results in a higher mean long-term growth rate across genotypes, while a stronger negative covariance reduces the mean long-term growth rate across genotypes (fig. 1A). When there is no nongenetic covariance, the fixed and uncorrelated condition matrices are the same and the mean long-term growth rate depends only on the expected values of the vital rates at each age. Importantly, the effects of nongenetic heterogeneity on the mean long-term growth rate can be larger than the effects of genetic heterogeneity, even when the variation in both is the same.

The sign of the genetic covariance has a consistent effect on evolvability, measured as the variance in long-term growth rates standardized by their mean squared (fig. 1B). Positive genetic covariances result in the highest evolvability because genotypes with a high mean survival probability and birth rate will replicate much faster than genotypes with a low mean survival probability and birth rate. Likewise, the lowest evolvability occcurs with negative genetic covariances because genotypes with high mean values of one vital rate will generally have low mean values of the other. Different genotypes will therefore tend to be more similar in their long-term growth rates, compared to positive covariances that allow for clearly superior and inferior genotypes. In further agreement, evolvability from the simulations with no genetic covariance falls in between the results from positive and negative genetic covariance.

Turning to nongenetic heterogeneity when vital rates are uncorrelated, the relative strength of nongenetic variation has no influence on evolvability (fig. 1B). Although the variation in survival and birth rates increases with the relative amount of nongenetic heterogeneity, it does so equally up (high fitness phenotypes) and down (low fitness phenotypes), and so the variance in long-term growth among genotypes should not change because the long-term growth rate depends only on the expectations of vital rates (which remain unchanged). This result also holds for fixed condition with no nongenetic covariance among vital rates. However, when the nongenetic covariance

is positive, increasing the relative strength of nongenetic heterogeneity always reduces evolvability with fixed condition. Indeed, the "lucky" individuals with high survival probabilities and high birth rates dominate more strongly as the strength of nongenetic heterogeneity increases; this results in part due to the "frailty effect" removing low condition phenotypes (Kendall et al. 2011; Vaupel et al. 1979) and in part due to an increase in vital rates for all high condition phenotypes. Accordingly, the lucky phenotypes for the different genotypes are more similar to one another in fitness and evolvability declines. The opposite effect occurs for negative nongenetic covariances among vital rates, where increasing the strength of nongenetic variation always increases the evolvability with fixed condition. With a negative nongenetic covariance, phenotypes tend to have either a high survival probability and low birth rate, or a low survival probability and high birth rate, causing the phenotypic heterogeneity to cancel out to some extent (i.e., all individuals are mediocre) and accentuating genotypic differences in long-term growth rates. Thus, unintuitively, the population evolves more quickly but towards a lower mean long-term growth rate as the strength of nongenetic heterogeneity is increased with a negative nongenetic covariance.

We next consider longer life spans, with reproduction only after 10 time steps (late recruitment). All else being equal, late recruitment reduces the long-term growth rate compared to early recruitment because individuals must survive longer before contributing to the population via reproduction (fig. 2A). Again, if the nongenetic heterogeneity is uncorrelated (dashed lines), the mean long-term growth rate is determined directly by the expectations of the survival probabilities and birth rates at each age, and so there is no influence of the sign of the nongenetic covariance. By contrast, the long-term growth rates are substantially higher when vital rates are fixed across the life span, increasingly so as the nongenetic heterogeneity in vital rates rises. In this case, there is a stronger frailty effect and the majority of phenotypes that survive long enough to reproduce are the "lucky" phenotypes with a high survival probability. With positive nongenetic covariance, this phenotype is also the one that tends to have high birth rates, allowing for the strongest increase in long-term growth rate with the strength of nongenetic heterogene-

ity. With negative nongenetic covariance, however, the individuals that are in the high survival probability phenotype will have the lowest birth rates, and so there is a slightly weaker increase in genotype fitness. The impact of the nongenetic covariance between survival and birth rates is, however, much more modest with late recruitment, because survival rates across all age classes are the same (i.e., survival at age a and $a+1$ are completely positively correlated).

As with early recruitment, the sign of the genetic covariance has a consistent effect on evolvability, where all else being equal, positive genetic covariances result in the highest evolvability and negative genetic covariances in the lowest evolvability (fig. 2B). Likewise, increasing the strength of nongenetic heterogeneity has no influence on the rate of evolution by natural selection when vital rates vary randomly over the lifespan. However, when the vital rates are fixed at birth, evolvability decreases as the relative strength of nongenetic variation increases; this is another consequence of only the few "lucky" individuals with high survival probabilities surviving long enough to reproduce, with genotypic differences being relatively modest.

This relatively simple example with uniformly distributed vital rates emphasizes the effects of nongenetic individual heterogeneity because all parameters are held constant across simulations, except the amount of nongenetic variation. However, vital rates will very rarely follow such a perfect distribution in natural populations. In more realistic situations, the processes generating nongenetic heterogeneity are likely to affect both the mean and variance of each vital rate, which will complicate the results depending on that relationship (e.g., Plard et al. 2016).

Discussion

Here we introduced phenotypic collapsing as a method that allows phenotypic heterogeneity in survival probabilities and birth rates to be captured within a traditional Leslie matrix, while preserving the full solution of the original full-scale model. Previous studies of matrix collapsing use a technique that typically enforces the same leading eigenvalue and stable age distribution as the original matrix (Hooley 2000; Salguero-Gómez and Plotkin 2010), however it need not capture

the left eigenvector associated with the leading eigenvalue (reproductive values) (Bienvenu et al. 2017; Coste et al. 2017) nor the remaining eigenstructure. Furthermore, by instead collapsing over the stable phenotype distribution as we do here (i.e., using the fraction of newborns that reach age a in phenotype x as collapsing weights, rather than the stable age distribution), we provide additional insight into the role that covariances between vital rates play in ecological and evolutionary dynamics. Our model is general in the sense that it makes no assumptions about the factors that generate and maintain variation in these vital rates, it allows for any number of age and phenotype classes, and it can be applied to a wide range of species, however it does require that the phenotype distribution is reset at birth, with randomly drawn juvenile phenotypes regardless of the parent's age or phenotype. While our simulations focus on the cases where vital rates are set at birth (fixed condition) or can vary randomly at anytime (uncorrelated condition), the theoretical analyses provide further insight by allowing for arbitrary phenotypic transitions across the lifespan, as will often be the case in natural populations (Orzack et al. 2011; Plard et al. 2012, 2018).

Our results emphasize the distinct influences of genetic and nongenetic variation in vital rates on ecological and evolutionary dynamics. In particular, we found that nongenetic individual heterogeneity can change a genotype's fitness and that this effect ultimately influences the mean long-term growth rate and evolvability among isolated genotypes, unless individual vital rates are reset randomly each time step (uncorrelated condition). Biologists should therefore be cautious using conventional evolutionary models that only consider the amount of genetic variation in a population.

Previous works support our result that nongenetic variation in vital rates can affect evolutionary dynamics. For example, Cressler et al. (2017) used an individual-based model to show that regardless of the sign of the nongenetic covariance among vital rates, rates of evolution by natural selection (calculated as the variance in genotypic growth rates) will always be slower with higher relative strengths of nongenetic individual heterogeneity. This model assumed fixed condition and that individuals had to survive at least ten time steps to reproduce, and so their findings cor-

respond to our special case of fixed condition and late recruitment (fig. 2B). Our study provides more general insight, however, as we find that evolvability can instead sometimes increase with the strength of nongenetic heterogeneity (as in the case where there is a trade-off among vital rates and early recruitment (fig. 1B)) or remain unchanged (e.g., with uncorrelated condition).

Quantitative genetics models have also found a diverse range of evolutionary consequences of nongenetic variation, from increasing a genotype's fitness and promoting adaptive evolution of the mean phenotype (Rocabert et al. 2020), to accelerating the rate of evolution despite decreasing average population fitness (Saito et al. 2013). This latter scenario matches our simulations with fixed condition and a nongenetic trade-off among vital rates (fig. 1), where increasing the magnitude of nongenetic variation allows evolution to proceed faster, yet it leads the population to a lower average fitness. While these observations seem counterintuitive considering Fisher's fundamental theorem (Fisher 1930), they may be at least partially explained by the idea of phenotypic subsidy driving reductions in average fitness: subsidies via birth from high condition phenotypes can prevent extinction of low condition phenotypes, and these low condition phenotypes can prevent high condition phenotypes from reaching the abundance that they otherwise would (Bolnick et al. 2011). Accordingly, when the relative strength of nongenetic individual heterogeneity is high in our model, phenotypic subsidies can maintain some phenotypes with particularly low survival probabilities or birth rates, increasing the variance in long-term growth rates among genotypes while simultaneously reducing their mean compared to when the nongenetic heterogeneity is relatively weaker.

Importantly, we find that the sign of the nongenetic covariance among individual survival probabilities and birth rates has a predictable influence on the long-term growth rate of a genotype. A similar effect was recognized by Stover et al. (2012), who incorporated fixed condition in birth and death rates into a logistic model with density-dependence in reproduction. The authors observed that a positive correlation among these vital rates (assumed to be independent of age) always increases the low-density population growth rate and equilibrium population size, while a negative correlation decreases both measures. Likewise, Kendall et al. (2011) found

that long-term population growth rates increase with the magnitude of heterogeneity in survival rates, which were held constant throughout life, creating a positive $Cov(l_a, s_a)$ in equation (16) (heterogeneity in birth rates had no effect in their model without a parent-offspring correlation, however, because it was uncorrelated with survival rates, so $Cov(l_a, b_a)$ were zero by assumption for all ages a). Here we expanded on the results of Kendall et al. (2011) and Stover et al. (2012) by explicitly considering genetic and nongenetic components of individual heterogeneity in vital rates in an age-structured model with an arbitrary number of phenotype classes and by exploring their consequences on evolvability. We also compare results to a model of dynamic condition, where individuals can change phenotypes throughout life.

The main result from our theoretical analysis showed that the long-term growth rate of a genotype depends on how vital rates do or do not vary throughout the life course. At one extreme, if vital rates vary randomly throughout the life course (uncorrelated condition), we find that population dynamics depend only on the average vital rates within an age class and are independent of any previous phenotypic history allowing suvival to that age (i.e., all covariances in equation (16) are 0). This finding corresponds to a study from Fox and Kendall (2002), which determined that if there is variability in vital rates but they are independent and identically distributed, then the influence of this heterogeneity on population dynamics disappears and the outcome matches what would be expected if all individuals had the same, average vital rate. All else being equal, we find that positive nongenetic covariances among survival up to an age class and the survival or birth rate at that age translate to greater genotypic fitness than expected if vital rates varied randomly throughout the life course, while trade-offs have the opposite effect (equation (16)). Under a positive covariance, individuals that have high survival probabilities also have high birth rates, and these "lucky" individuals substantially increase genotype fitness throughout their lives. In natural populations of the parlour palm and rainforest trees, for example, high condition individuals contribute up to 2.4 times as much to population growth rates as low condition individuals (Jansen et al. 2012; Zuidema et al. 2009). However, trade-offs are also widespread in nature and they occur when individuals that have a high survival probability pay

a cost with a low birth rate or vice versa (e.g., Dahlgren et al. 2016; Gould et al. 2018; Lemaître et al. 2015). Trade-offs are expected to provide higher fitness when life histories are dynamic because individuals that have a high survival probability at one time can potentially move among phenotypes and have a high birth rate at the next (Supplemental material S1).

Whether the covariances are positive or negative, the model predicts that vital rate heterogeneity will have a stronger effect in the life-history stages where phenotypes are longer-lived (leading to stronger covariances). For example, if transitions are dynamic early in life, but fixed (highly correlated) later (perhaps after development), then the covariance among vital rates would be expected to have a much larger effect at older ages. This result corresponds with a recent study from Bliard et al. (2024), which found that populations with longer lifespans are more sensitive to changes in the strength of vital rate trade-offs because cohort selection has more opportunities to take place than in populations with shorter lifespans. Our finding also implies that even when covariances among survival probabilities and birth rates are expected to be strong, their impacts on population dynamics may be masked by frequent transitions among phenotypes. Similarly, Lee et al. (2017) found that reproductive autocorrelations (as would be produced in our models of fixed or dynamic condition) have a stronger effect on the demographic variance and stochastic population growth rate when females have a low probability of switching reproductive status as they age. Our framework could therefore explain why previous studies have found that heterogeneity has only a weak effect on the variance among individual longevity and lifetime reproductive success compared to stochasticity in vital rates (Hartemink and Caswell 2018; Jenouvrier et al. 2018; Snyder and Ellner 2018; Steiner and Tuljapurkar 2012): the effects of heterogeneity are hidden by frequent transitions occurring under stochasticity.

These effects of the sign of the nongenetic covariance among vital rates on a single genotype scale up to determine the mean long-term growth rate among multiple co-evolving genotypes (fig. 1A). In the simple case of two age classes ("early recruitment"), the effect of the covariance among vital rates on population dynamics is most distinct and the mean long-term growth rate is greater for fixed condition when nongenetic covariances are positive, but greater for uncorrelated

condition when nongenetic covariances are negative. In agreement, simulations from an individual based model of fixed condition (Cressler et al. 2017) showed that increasing the strength of nongenetic variation increases genotype growth rates when nongenetic covariances are positive, while negative covariances have the opposite effect. Our analytical results thus explain how the sign and magnitude of the nongenetic covariance among vital rates determines genotype growth rates in Cressler et al. (2017).

In contrast, if individuals have longer development times ("late recruitment"), we observed that fixed condition always results in higher mean long-term growth rates than uncorrelated condition and that this difference increases with the strength of nongenetic heterogeneity (fig. 2A). Fixed condition means that individuals that are born with a high survival probability are guaranteed to maintain that high survival probability throughout their life. If instead vital rates are dynamic, individuals that have a high survival probability at one time may transition and have a low survival probability at the next; it is therefore less likely that individuals will survive to reproduce and genotype fitness will generally be lower than with fixed condition. This result emphasizes the importance of heterogeneity for long-lived species, where maturity generally occurs later in life and so cohort selection within a generation has more time to remove the weaker individuals and leave only those with a sufficiently high survival probability to reproduce (Bliard et al. 2024; Kendall et al. 2011; Lloyd et al. 2020; Vaupel and Yashin 1985). If phenotypes were heritable, this kind of selection could be advantageous as offspring would inherit, on average, higher survival probabilities than those of their parents. Still, our simulations assumed constant vital rate expectations and transition probabilities. The nuances of the type of individual heterogeneity, the vital rate distributions, the sign of the (non)genetic covariance, and the number of age classes can generate a wide range of ecological and evolutionary dynamics across populations.

Interestingly, we found only a small influence of the sign of the genetic covariance on the mean long-term growth rate among genotypes. This result is also similar to the results of Cressler et al. (2017), who found that the mean genotype growth rate is sensitive to the sign of the nongenetic covariance among vital rates, but largely insensitive to the genetic covariance

structure. Overall, these findings emphasize that long-term growth rates and evolvability can depend equally, if not more, strongly on nongenetic (co)variances as genetic.

Historically, a substantial barrier to incorporating individual heterogeneity in theoretical models has been the cost of added complexity when individuals cannot be considered identical. Here, we applied matrix collapsing (Enright et al. 1995; Hooley 2000) to reduce population projection matrices with an arbitrary number of phenotypes and ages to a standard Leslie matrix, while maintaining the complete solution of the original full-scale matrix, after a short delay (of at most ω time steps) so that no individuals remain alive from the initial population (whose configuration was arbitrary). For the first time (to our knowledge), we have identified certain kinds of matrices that can be collapsed using phenotypic collapsing and still preserve the full solution of the original model. This work builds on previous theory that has developed collapsing methods that capture all asymptotic properties of the matrix (e.g., Bienvenu et al. 2017, Coste et al. 2017), but unlike our approach, do not necessarily preserve the transient dynamics for all times $t \geq \omega$. Another advantage of phenotypic collapsing is that the collapsing weights are calculated using only matrix powers and the distribution of juvenile phenotypes (see Appendix 1), which are generally much easier to compute for large matrices than the eigenvectors required in previous methods. This collapsed matrix can be used in future theoretical and empirical studies to consider variation in mortality and birth rates without sacrificing model accuracy.

The collapsed matrix also provides insight about when among-individual variation in vital rates can be ignored in studies of population dynamics to avoid unnecessary complexity (see Appendix 2 below). Equation (A2.1) shows that empirical researchers can accurately predict population dynamics using only average age-specific vital rates, even when there is nongenetic heterogeneity in those vital rates within each age class. As long as researchers ensure random sampling and as long as the phenotypic distribution at each age is stable (e.g., the projection matrix is of the form of equation (15) and has been stable since birth), all of the ways to survive up to an age class and then have a particular survival probability or birth rate at that age will be accounted for in the expected values of the vital rates. For instance, previous simulations

that used an IPM to account for variation in survival and fecundity found no influence of this heterogeneity on the asymptotic population growth rate when compared to the same population analyzed with an IPM ignoring such variation (Vindenes and Langangen 2015). This method will be sufficient for many population-level studies, however it will fail if the goal of the analysis is to measure variability among life histories and its influence on demographic parameters. The matrix in equation (16) directly incorporates all of the life history paths that an individual could follow throughout its life course and highlights the importance of the covariance between an individual's history and its current phenotype in determining population dynamics.

Our simulations reveal that populations may face a trade-off between growing faster (i.e., having the greatest mean long-term growth rate) and evolving faster (fig. 1; fig. 2). Indeed, if life-histories are fixed condition, we found that increasing the magnitude of nongenetic heterogeneity benefits the mean long-term growth rate when it reduces evolvability and vice-versa. Thus, populations consisting of individuals with permanent vital rates may have an advantage for growth in a constant environment but may not be able to adapt as quickly in the face of environmental change. Future work should ask whether such environmental fluctuations influence the type of individual heterogeneity that is found across real populations.

Here we have shown that nongenetic individual heterogeneity in vital rates can influence genotype fitness as well as the mean long-term growth rate and evolvability in populations of isolated genotypes. We restricted our analyses to density-independent age-structured models to isolate the consequences of nongenetic (co)variation as much as possible, however we expect that nongenetic heterogeneity will generally affect ecological and evolutionary dynamics. One limitation of our method is that we assumed no parent-offspring correlations. Relaxing this assumption would allow the model to account for various degrees of nongenetic heritability and for potential negative correlations in the vital rates of parents and offspring (e.g., due to density effects or spatial heterogeneity), although it is important to note that the collapsed population projection matrices would be different from those that we have shown here and would not necessarily maintain the characteristic polynomial, reproductive values, or transient population dynamics.

To add further biological realism, influences of environmental stochasticity (Engen et al. 2007; Sæther and Engen 2015), and continuous variation in vital rates (Plard et al. 2018; Vindenes and Langangen 2015) could also be considered. While the precise effects of the type of individual heterogeneity and nongenetic (co)variance would be less clear, these models may provide more accurate predictions of growth rates and evolvability in real populations. Our results emphasize the importance of not only considering among-individual variation in vital rates, but also the structure of that variation (e.g., genetic or nongenetic, fixed or dynamic condition, positive or negative covariance), when making predictions about ecological and evolutionary processes.

Acknowledgments

We would like to thank Dr. Ophélie Ronce for feedback that improved this version of the manuscript and Dr. Christophe Coste for insights about matrix collapsing. This work was supported by the Natural Sciences and Engineering Council of Canada (graduate scholarships to ABF (CGS-M and CGS-D) and Discovery Grants to TD (NSERC RGPIN-2022-03362) and SPO (NSERC RGPIN-2022-03726)) and the University of British Columbia (Four Year Doctoral Fellowship to ABF).

Statement of Authorship

ABF, TD and WAN conceptualized the work and developed the models. ABF performed model analysis, developed the R code, and carried out the simulations with substantial input from SPO and TD. SPO wrote the first draft of the *Mathematica* code (edited and finalized by ABF). ABF wrote the original draft of the manuscript with input from SPO and TD and all authors contributed to editing and revisions.

Appendix 1: A proof for phenotypic collapsing

Notation and set up: The model is $\vec{N}(t+1) = \mathbf{L}_{\rho,\omega}\vec{N}(t)$ where $\vec{N}(t)$ is a vector whose elements $n_{x,a}$ indicate the number of individuals in phenotype x at age a and $\vec{N}(0)$ is the initial condition at time $t = 0$. We can decompose $\mathbf{L}_{\rho,\omega}$ as $\mathbf{L}_{\rho,\omega} = \mathbf{F} + \mathbf{V}$ where $\mathbf{F}$ is a square ferility matrix of dimension $\rho \cdot \omega$ and contains the first ρ rows of $\mathbf{L}_{\rho,\omega}$ and zeros eleswhere, and $\mathbf{V} = \mathbf{L}_{\rho,\omega} - \mathbf{F}$. Notice that $\mathbf{V}$ is a block subdiagonal matrix that tracks the survival of individuals. $\mathbf{V}$ consists of $\omega - 1$ blocks and so it is nilpotent of degree ω (i.e., $\mathbf{V}^{\tau} = 0$ for all integral powers $\tau \geq \omega$). We focus on cases where the probability that a juvenile starts in phenotype x is j_x, independent of the parental age, phenotype, or genotype. The probability distribution of these newborns is given by the vector $\vec{j} = [j_1, \cdots, j_\rho, 0, \cdots 0]$ whose first ρ elements give the fraction of offspring born in phenotype x and whose remaining $\rho \cdot (\omega - 1)$ elements are zeros. Define $n_a(t) = \sum_{x=1}^{\rho} n_{x,a}(t)$ to be the total number of individuals of age a at time t, $\vec{N}_C(t)$ with elements $n_a(t)$ to be the ω-dimensional vector describing the total number of individuals in each age class, and $\psi_{x,a}(t) = \dfrac{n_{x,a}(t)}{n_a(t)}$ to be the fraction of age a individuals at time t that have phenotype x.

Theorem: Consider the $\rho \cdot \omega$ dimensional initial value problem $\vec{N}(t+1) = \mathbf{L}_{\rho,\omega}\vec{N}(t)$ with initial vector at time $t = 0$ given by $\vec{N}(0)$. The solution $\vec{N}(t)$ for time $t \geq \omega$ is completely described by the solution of the reduced, ω dimensional initial value problem $\vec{N}_C(t+1) = \mathbf{L}_{\omega}\vec{N}_C(t)$ with initial vector at time $t = \omega$ given by $\vec{N}_C(\omega)$ and where the elements of $\mathbf{L}_{\omega}$ are block averages over time-invariant values of $\psi_{x,a}(t)$ defined by $\psi_{x,a} = \dfrac{[\mathbf{V}^{a-1}\vec{j}]_{x,a}}{\mathbf{V}^{a-1}\vec{j} \cdot \vec{1}}$ where $[\mathbf{V}^{a-1}\vec{j}]_{x,a}$ is the x, ath entry of the vector given by $\mathbf{V}^{a-1}\vec{j}$ and $\vec{1}$ is a $\rho \cdot \omega$ dimensional vector of ones.

Proof: Consider the collapsed matrix $\mathbf{L}_{\omega}$ obtained by averaging the elements of $\mathbf{L}_{\rho,\omega}$ over the phenotypic distribution $\psi_{x,a}(t)$ for each age class a. Only if $\psi_{x,a}(t)$ is time invariant will $\vec{N}_C(t+1) = \mathbf{L}_{\omega}\vec{N}_C(t)$ represent a linear system of equations involving the ω entries of $\vec{N}_C(t)$, describing the total number of individuals in each age class. Here we will show that, for times $t \geq \omega$ these $\psi_{x,a}(t)$ are in fact time invariant and given by $\psi_{x,a} = \dfrac{[\mathbf{V}^{a-1}\vec{j}]_{x,a}}{\mathbf{V}^{a-1}\vec{j} \cdot \vec{1}}$. Thus for $t \geq \omega$, the solution of the original model lies in the ω-dimensional subspace spanned by the eigenvalues and eigenvectors

of the collapsed model. In other words, for any time $t \geq \omega$, the matrix $\mathbf{L}_\omega$ obtained from phenotypic collapsing completely predicts the dynamics of the original full matrix, even if the stable age distribution has not yet been reached.

We begin by writing the solution $\vec{N}(t)$ in renewal form as $\vec{N}(t) = \mathbf{V}^t\vec{N}(0) + \sum_{\tau=1}^{t} \mathbf{V}^{\tau-1}\vec{R}(t-\tau)$ for $t \geq 1$ where $\vec{R}(t-\tau)$ is a vector whose first ρ elements are the total recruitment of offspring of phenotype x, by all individuals present at time $t-\tau$, and whose remaining elements are zeros. Because $\mathbf{V}$ is nilpotent of degree ω, for times $t \geq \omega$ we have $\vec{N}(t) = \sum_{\tau=1}^{\omega} \mathbf{V}^{\tau-1}\vec{R}(t-\tau)$. Furthermore, because there is no inheritance of parent phenotypes, $\vec{R}(t-\tau) = \vec{j}\,b_{t-\tau}$ where $b_{t-\tau}$ is a scalar giving the total number of new recruits of age one individuals of all phenotypes by all individuals present at time $t-\tau$. Therefore, $\vec{N}(t) = \sum_{\tau=1}^{\omega} \mathbf{V}^{\tau-1}\vec{j}\,b_{t-\tau}$ for $t \geq \omega$. Notice that the time dependence, t, appears only in $b_{t-\tau}$. Finally, it can be checked that because of the form of $\mathbf{V}$ and $\vec{j}$, the terms $\mathbf{V}^{\tau-1}\vec{j}\,b_{t-\tau}$ in the summation of $\sum_{\tau=1}^{\omega} \mathbf{V}^{\tau-1}\vec{j}\,b_{t-\tau}$ are each a vector with zeros everywhere except for the block corresponding to age τ. Therefore, $n_a(t) = \mathbf{V}^{a-1}\vec{j}\,b_{t-a} \cdot \vec{1}$ and $n_{x,a}(t) = [\mathbf{V}^{a-1}\vec{j}\,b_{t-a}]_{x,a}$. Thus after simplifying,

$$\psi_{x,a} = \frac{[\mathbf{V}^{a-1}\vec{j}]_{x,a}}{\mathbf{V}^{a-1}\vec{j} \cdot \vec{1}} \tag{A1.1}$$

which is independent of time t.

Recipe: Define $\mathbf{A}$ to be an $\omega \times (\rho \cdot \omega)$ matrix with rows for each age class a (in order from 1 to ω) that contain ρ ones in the slot for age class a and zeros elsewhere. Define $\mathbf{B}$ to be a $(\rho \cdot \omega) \times \omega$ matrix with columns for each age class a (in order from 1 to ω) containing the collapsing weights, $\psi_{x,a}$ for each age a and zeros elsewhere. The collapsed matrix is then given by

$$\mathbf{L}_\omega = \mathbf{A}\mathbf{L}_{\rho,\omega}\mathbf{B} \tag{A1.2}$$

Notice that the matrices $\mathbf{A}$ and $\mathbf{B}$ follow the same structure as $\mathbf{P}$ and $\mathbf{Q}$ (respectively) in the collapsing method of Hooley (2000), but with entries that collapse over phenotypes instead of age classes and with collapsing weights $\psi_{x,a}$ determined by the stable phenotype distribution rather than the stable age and phenotype distribution. A major advantage of phenotypic collapsing is that these weights ($\psi_{x,a}$, equation (A1.1)) can be calculated using only matrix powers (of the

survival matrix, $\mathbf{V}$) and the distribution of juvenile phenotypes ($\vec{j}$). Previous collapsing methods on the other hand (e.g., Bienvenu et al. 2017; Coste et al. 2017; Hooley 2000) require an eigenanalysis of the orginial, full-scale matrix to calculate the collapsing weights (typically determined by the dominant eigenvalue and eigenvector pair), and these computations become challenging to compute analytically or even numerically for very large matrices.

Appendix 2: Some properties of phenotypic collapsing

First, notice that for all times $t \geq \omega$ the collapsing weights given by $\psi_{x,a}$ are simply the probability that an individual is in phenotype x at age a, given that it survived to age a. Thus we can also write $\psi_{x,a} = \dfrac{E[l_{x,a}]}{E[l_a]}$ where $E[l_{x,a}]$ is the expected probability of lifetime survival, from a random juvenile phenotype leading up to an age a individual in phenotype x, calculated over the possible juvenile distribution. Specifically, let $l^i_{x,a} = j_{x_1} \prod_{k=1}^{a-1} f_{x_k \to y_{k+1}} s_{x,k}$ represent one of several possible paths i that an individual born with phenotype x_1 could take to survive and express phenotype $x_a = x$ at age a, considering all of the phenotypes x_k that the individual experienced between birth and age a. The sum over all of these paths $\sum_{i=1}^{paths} l^i_{x,a} = E[l_{x,a}]$ gives a weighted average of all potential phenotypic transitions leading an individual to phenotype x at age a (where the weights are determined by the transition probabilities that determine how likely each path is); this summation is an alternative mathematical expression of $[\mathbf{V}^{a-1}\vec{j}]_{x,a}$. The sum over all paths and phenotypes $\sum_{x=1}^{\rho} \sum_{i=1}^{paths} l^i_{x,a} = E[l_a]$ gives a weighted average of all of the ways that an individual can survive to age a, considering all of the phenotypes x that it could express at that age, which is equivalent to $\mathbf{V}^{a-1}\vec{j} \cdot \vec{1}$. These entries $\psi_{x,a}$ of the stable phenotype distribution can be put together into the vector $\vec{\psi}$, which gives the stationary proportion of individuals in each phenotype x for each age a. As it turns out, the stationary phenotypic proportions for each age given in $\vec{\psi}$ are the same as would be obtained at the stable age *and* phenotype distribution (given by the right eigenvector associated with the leading eigenvalue of $\mathbf{L}_{\rho,\omega}$), however our methods do not require that the stable age distribution has been reached.

Our application of matrix collapsing uses this stable phenotype distribution to collapse all of the phenotypes within each age class to a single, effective phenotype for that age class. The weightings for each phenotype x at age a are given by $\psi_{x,a}$ as defined above and in Appendix 1. The effective vital rates are then given by $\frac{\sum_{x=1}^{\rho} E[l_{x,a} r_{x,a}]}{E[l_a]} = \frac{E[l_a r_a]}{E[l_a]}$ where r is one of the two vital rates (survival probability or birth rate), and $E[l_a r_a]$ gives an expected value of the vital rate at age a, considering all of the potential phenotypes that could be expressed at age a and all of the possible life histories (i.e., phenotypic transitions and survival probabilities) that an individual could have experienced as it survives up to that age.

Recalling that for any variables x and y the expected value $E[xy]$ can be written in terms of the covariance, $E[xy] = E[x]E[y] + Cov(x, y)$, we now seek to define what these expectations should be if there were no covariance. If the current vital rates did not depend on previous vital rates, we could obtain the phenotypic distribution at age a as above, but ignoring previous survival rates. Hence, we define $t^i_{x,a} = j_{x_1} \prod_{k=1}^{a-1} f_{x_k \to x_{k+1}}$ to be the probability of the path i for an individual born in phenotype x_1, considering all of the phenotypes x_k that it transitions through to express phenotype $x_a = x$ at age a, as if differences in survival rates at previous ages did not affect the current vital rates. Setting the survival probabilities to one in the survival matrix $\mathbf{V}$ (as defined in Appendix 1), we get a matrix that we call $\mathbf{V_T}$ and $t^i_{x,a}$ can be calculated from the entries of ${\mathbf{V_T}}^{a-1} \cdot \vec{j}$ (note that the transition probability of all possible paths from birth to age a sum to one for each age a, i.e., $\sum_{x=1}^{\rho} \sum_{i=1}^{paths} t^i_{x,a} = 1$). Defining $\sum_{i=1}^{paths} t^i_{x,a} = E[t_{x,a}]$ and $E[r_a] = \sum_{x=1}^{\rho} E[t_{x,a} r_{x,a}]$, the collapsed ω-age matrix can then be written as in equation (16).

As an alternative, we note that equation (16) can also be written as

$$\mathbf{L}_\omega = \begin{bmatrix} E^*[b_1] & E^*[b_2] & E^*[b_3] & \cdots & E^*[b_{\omega-1}] & E^*[b_\omega] \\ E^*[s_1] & 0 & 0 & \cdots & 0 & 0 \\ 0 & E^*[s_2] & 0 & \cdots & 0 & 0 \\ 0 & 0 & E^*[s_3] & \cdots & 0 & 0 \\ \vdots & \vdots & \vdots & \ddots & \vdots & \vdots \\ 0 & 0 & 0 & \cdots & E^*[s_{\omega-1}] & 0 \end{bmatrix} \tag{A2.1}$$

where the expectations, E^*, are taken over over all of the possible phenotypic histories that an individual could have experienced to survive to age a, accounting for both the transition and survival probabilities encountered along the way, that is, defining $E^*[r_a] = \dfrac{E[l_a r_a]}{E[l_a]}$. This form of the collapsed matrix shows that empirical estimates of age-specific vital rates are accurate, even when there is heterogeneity in the vital rates within each age class, as long as there is random sampling and the population is at the stable phenotype distribution, as expected if the vital rates have remained constant for $t \geq \omega$ timesteps. This alternative form of the collapsed matrix, however, hides the impact of phenotypic heterogeneity and the covariance among vital rates on the growth of the population, as revealed by equation (16).

As argued here and in Appendix 1 (see also worked examples in Supplemental material S2) the stable phenotypic distribution $\vec{\psi}$ is attained within a single generation, once no individuals remain alive from the initial population ($t \geq \omega$). Consequently, as long as the juvenile distribution does not depend on the parental age and phenotype, the collapsed matrix, alongside the time invariant phenotypic distribution $\vec{\psi}$, fully describes the future state of the system for all $t \geq \omega$. The solution of the original model with the matrix $\mathbf{L}_{\rho,\omega}$ is therefore simply a linear combination of the eigenvalues and eigenvectors associated with the collapsed matrix $\mathbf{L}_\omega$ (see Supplemental material S2 for an example). In a forthcoming article we will derive the explicit relationship between the eigensolutions of the full and the reduced system and explore more generally the kinds of matrix models that can be simplified using phenotypic collapsing. This implies that the characteristic polynomials of the collapsed and original ρ-phenotype ω-age matrix are propor-

tional to one another and exactly equal when put in Euler-Lotka form (see Supplemental material S2 for an example). The Euler-Lotka equation (Euler 1760; Sharpe and Lotka 1911) is given by setting the characteristic polynomial equal to zero and rearranging terms such that

$$1 = \sum_{a=1}^{\omega} l_a b_a \lambda^{-a} \tag{A2.2}$$

where l_a is the proportion of individuals surviving to age a and b_a is the average number of offspring born to an individual of age a, assuming that the population is at its stable age distribution. This equation reveals that the average lifetime reproductive output for individuals is the sum of all age-specific contributions to fitness, via births and survival.

The characteristic polynomial for the collapsed matrix with heterogeneity is

$$\begin{aligned} 1 = {} & E[b_1]\lambda^{-1} + \left(Cov(l_2, b_2) + E[l_2]E[b_2]\right)\lambda^{-2} + \left(Cov(l_3, b_3) + E[l_3]E[b_3]\right)\lambda^{-3} \\ & + \cdots + \left(Cov(l_\omega, b_\omega) + E[l_\omega]E[b_\omega]\right)\lambda^{-\omega} \end{aligned} \tag{A2.3}$$

This equation further emphasizes the influence of the covariance among vital rates on population growth when individual life histories have at least some phenotypic "memory." All else being equal, the average contribution of an age class to lifetime reproductive output can be higher (positive covariance), lower (negative covariance), or the same (no covariance) as if the phenotypes were randomly assigned.

While the phenotypic distribution described by $\vec{\psi}(t)$ holds immediately for all $t \geq \omega$, the stable age distribution will often take several generations to be approached. A major advantage of phenotypic collapsing is that it does not assume that the population is at a stable age distribution and therefore the collapsed matrix $\mathbf{L}_\omega$ can still describe transient dynamics as the age structure stabilizes (Appendix 1; see examples in Supplemental material S2). Here we briefly consider the stable age distribution with phenotypic collapsing (see worked examples in Supplemental material S2). The entries of the stable age distribution for age a in the collapsed matrix $\mathbf{L}_\omega$ are given by the expected value of survival to age a, $E[l_a]$, as described by summing all of the paths from birth to age a accounting for all possible phenotypic transitions (equivalently by $\mathbf{V}^{a-1}\vec{j} \cdot \vec{1}$). Notice that these entries of the stable age distribution of the collapsed matrix are simply the sum

of the entries of the stable age and phenotype distribution from the original matrix $\mathbf{L}_{\rho,\omega}$

$$\begin{aligned}\widetilde{u_{\cdot a}} &= \sum_{x=1}^{\rho} \psi_{x,a} E[l_a] \\ &= E[l_a]\end{aligned} \tag{A2.4}$$

Equation (A2.4) falls in agreement with previous studies of matrix collapsing, which find that the entries of the stable age or stage distribution of the original matrix (in this case, the entries of the stable age and phenotype distribution of $\mathbf{L}_{\rho,\omega}$) can be summed over the collapsed classes to calculate the entries of the stable (st)age distribution for the collapsed matrix (Hooley 2000; Salguero-Gómez and Plotkin 2010).

Previous studies of matrix collapsing (which use the stable (st)age distribution as collapsing weights) guarantee that the dominant eigenvalue and its associated right eigenvector from the original matrix will be captured in the collapsed matrix. However, in contrast to phenotypic collapsing, even the left eigenvector associated with the dominant eigenvalue (which gives the reproductive value of each class) is only captured in particular cases with this method. For example, a study from Coste et al. (2017) found that matrix collapsing over the stable state distribution can capture reproductive values for matrices where the "contributions from all states (or future states) are equally broken down with regards to the soon-to-be-grouped states" (Coste et al. 2017). The matrices that we use here fit this condition because the heterogeneity is "reset" at the newborn stage when there is no inheritance of parental phenotypes (Coste pers. comm.); this implies that the age-specific reproductive values are the same before and after collapsing, if they are weighted by the stable phenotype distribution. The age-specific reproductive values, $\widetilde{v_{\cdot a}}$, of the collapsed ω-age matrix are therefore given by

$$\widetilde{v_{\cdot a}} = \sum_{x=1}^{\rho} v_{x,a} \psi_{x,a} \tag{A2.5}$$

where the reproductive values of the original ρ-phenotype ω-age matrix, $v_{x,a}$, indicate the asymptotic contributions of an individual in each age-and-phenotype specific class to future generations, relative to individuals in other classes (see worked examples in Supplemental material 2). The reproductive values of each age class in the collapsed matrix are therefore proportional

to the reproductive values of the ρ phenotypes that were merged to form that age class from the original ρ-phenotype ω-age matrix. Weighting by $\psi_{x,a}$ ensures that the contribution of each age class to future generations is scaled by the proportion of individuals that are expected in each phenotype class in the long run. Equation (A2.5) is also in agreement with the form of reproductive values from Bienvenu et al. (2017), who developed a different collapsing technique ("genealogical collapsing") that always captures the asymptotic population growth rate, as well as both its associated right and left eigenvectors from the original full matrix. Note, however, that the weightings applied to the reproductive values by Bienvenu et al. (2017) assume that the population is at its stable stage distribution (given by the right eigenvector associated with the dominant eigenvalue), whereas the weightings we use only require that the population is at a stable phenotype distribution, which is obtained once $t \geq \omega$ and all individuals in the population develop from juveniles drawn from the same $\vec{j}$. Furthermore, with phenotypic collapsing, the general solution and therefore the full nonzero eigensystem is captured, not just the leading eigenvalue and its associated eigenvectors. Thus, the future dynamics of the system are fully predicted, without assuming that the system is at the stable age distribution.

Code Availability

All R code for performing simulations and generating figures is available in the Dryad Digital Repository (`https://datadryad.org/stash/share/8Yh2oLMu4BXHhrurxgKfd1DEZjM2BqvteGyeyCQ4tz8`, Forsythe et al. 2024).

Literature Cited

Acker, P., A. Robert, R. Bourget, and B. Colas. 2014. Heterogeneity of reproductive age increases the viability of semelparous populations. Functional Ecology 28:458–468.

Armstrong, D. P., M. G. Keevil, N. Rollinson, and R. J. Brooks. 2018. Subtle individual variation in indeterminate growth leads to major variation in survival and lifetime reproductive output in a long-lived reptile. Functional Ecology 32:752–761.

Badger, J. J., W. D. Bowen, C. E. den Heyer, and G. A. Breed. 2020. Variation in individual reproductive performance amplified with population size in a long-lived carnivore. Ecology 101:e03024.

Beckage, B., and J. S. Clark. 2003. Seedling survival and growth of three forest tree species: the role of spatial heterogeneity. Ecology 84:1849–1861.

Benton, T. G., S. J. Plaistow, and T. N. Coulson. 2006. Complex population dynamics and complex causation: devils, details and demography. Proceedings of the Royal Society B: Biological Sciences 273:1173–1181.

Bienvenu, F., E. Akçay, S. Legendre, and D. M. McCandlish. 2017. The genealogical decomposition of a matrix population model with applications to the aggregation of stages. Theoretical Population Biology 115:69–80.

Bliard, L., M. Paniw, D. Z. Childs, and A. Ozgul. 2024. Population dynamic consequences of context-dependent tradeoffs across life histories. The American Naturalist [Forthcoming].

Bolnick, D. I., P. Amarasekare, M. S. Araújo, R. Bürger, J. M. Levine, M. Novak, V. H. W. Rudolf, S. J. Schreiber, M. C. Urban, and D. A. Vasseur. 2011. Why intraspecific trait variation matters in community ecology. Trends in Ecology & Evolution 26:183–192.

Bonduriansky, R., and T. Day. 2009. Nongenetic inheritance and its evolutionary implications. Annual Review of Ecology, Evolution, and Systematics 40:103–125.

———. 2018. Extended heredity: a new understanding of inheritance and evolution. Princeton University Press, Princeton.

Bonnet, T., and E. Postma. 2016. Successful by chance? The power of mixed models and neutral simulations for the detection of individual fixed heterogeneity in fitness components. The American Naturalist 187:60–74.

Bonnet, T., P. Wandeler, G. Camenisch, and E. Postma. 2017. Bigger is fitter? Quantitative genetic decomposition of selection reveals an adaptive evolutionary decline of body mass in a wild rodent population. PLOS Biology 15:e1002592.

Bright Ross, J. G., C. Newman, C. D. Buesching, and D. W. Macdonald. 2020. What lies beneath? Population dynamics conceal pace-of-life and sex ratio variation, with implications for resilience to environmental change. Global Change Biology 26:3307–3324.

Broekman, M. J. E., E. Jongejans, and S. Tuljapurkar. 2020. Relative contributions of fixed and dynamic heterogeneity to variation in lifetime reproductive success in kestrels (*Falco tinnunculus*). Population Ecology 62:408–424.

Bruijning, M., E. Jongejans, and M. M. Turcotte. 2019. Demographic responses underlying eco-evolutionary dynamics as revealed with inverse modelling. Journal of Animal Ecology 88:768–779.

Cam, E., L. M. Aubry, and M. Authier. 2016. The conundrum of heterogeneities in life history studies. Trends in Ecology & Evolution 31:872–886.

Cam, E., B. Cadiou, J. E. Hines, and J. Y. Monnat. 2002. Influence of behavioural tactics on recruitment and reproductive trajectory in the kittiwake. Journal of Applied Statistics 29:163–185.

Cam, E., O. Gimenez, R. Alpizar-Jara, L. M. Aubry, M. Authier, E. G. Cooch, D. N. Koons, W. A. Link, J.-Y. Monnat, J. D. Nichols, J. J. Rotella, J. A. Royle, and R. Pradel. 2013. Looking for

a needle in a haystack: inference about individual fitness components in a heterogeneous population. Oikos 122:739–753.

Caswell, H. 2001. Matrix population models: construction, analysis, and interpretation. Sinauer Associates, Sunderland.

Chambert, T., J. J. Rotella, and R. A. Garrott. 2014. An evolutionary perspective on reproductive individual heterogeneity in a marine vertebrate. Journal of Animal Ecology 83:1158–1168.

Chambert, T., J. J. Rotella, M. D. Higgs, and R. A. Garrott. 2013. Individual heterogeneity in reproductive rates and cost of reproduction in a long-lived vertebrate. Ecology and Evolution 3:2047–2060.

Clutton-Brock, T. H., M. Major, S. D. Albon, and F. E. Guinness. 1987. Early development and population dynamics in red deer. I. Density-dependent effects on juvenile survival. The Journal of Animal Ecology 56:53–67.

Cooper, E. B., and L. E. B. Kruuk. 2018. Ageing with a silver-spoon: a meta-analysis of the effect of developmental environment on senescence. Evolution Letters 2:460–471.

Coste, C. F. D., F. Austerlitz, and S. Pavard. 2017. Trait level analysis of multitrait population projection matrices. Theoretical Population Biology 116:47–58.

Coste, C. F. D., and S. Pavard. 2020. Analysis of a multitrait population projection matrix reveals the evolutionary and demographic effects of a life history trade-off. Ecological Modelling 418:108915.

Coulson, J. C. 1968. Differences in the quality of birds nesting in the centre and on the edges of a colony. Nature 217:478–479.

Coulson, J. C., and J. M. Porter. 1985. Reproductive success of the kittiwake *Rissa tridactyla*: the roles of clutch size, chick growth rates and parental quality. Ibis 127:450–466.

Coulson, T., T. G. Benton, P. Lundberg, S. R. X. Dall, B. E. Kendall, and J.-M. Gaillard. 2006. Estimating individual contributions to population growth: evolutionary fitness in ecological time. Proceedings of the Royal Society B: Biological Sciences 273:547–555.

Cressler, C. E., S. Bengtson, and W. A. Nelson. 2017. Unexpected nongenetic individual heterogeneity and trait covariance in *Daphnia* and its consequences for ecological and evolutionary dynamics. The American Naturalist 190:E13–E27.

Dahlgren, J. P., F. Colchero, O. R. Jones, D.-I. Øien, A. Moen, and N. Sletvold. 2016. Actuarial senescence in a long-lived orchid challenges our current understanding of ageing. Proceedings of the Royal Society B: Biological Sciences 283:20161217.

Danchin, É., A. Charmantier, F. A. Champagne, A. Mesoudi, B. Pujol, and S. Blanchet. 2011. Beyond DNA: integrating inclusive inheritance into an extended theory of evolution. Nature Reviews Genetics 12:475–486.

Day, T., and R. Bonduriansky. 2011. A unified approach to the evolutionary consequences of genetic and nongenetic inheritance. The American Naturalist 178:E18–E36.

Deere, J. A., T. Coulson, S. Cubaynes, and I. M. Smallegange. 2017. Unsuccessful dispersal affects life history characteristics of natal populations: the role of dispersal related variation in vital rates. Ecological Modelling 366:37–47.

Descamps, S., J.-M. Gaillard, S. Hamel, and N. G. Yoccoz. 2016. When relative allocation depends on total resource acquisition: implication for the analysis of trade-offs. Journal of Evolutionary Biology 29:1860–1866.

Dierickx, E. G., R. A. Robinson, and M. d. L. Brooke. 2019. Survival of a long-lived single island endemic, the Raso lark *Alauda razae*, in relation to age, fluctuating population and rainfall. Scientific Reports 9:19557.

Douhard, M., J.-M. Gaillard, D. Delorme, G. Capron, P. Duncan, F. Klein, and C. Bonenfant. 2013.

Variation in adult body mass of roe deer: early environmental conditions influence early and late body growth of females. Ecology 94:1805–1814.

Dudeck, B. P., M. Clinchy, M. C. Allen, and L. Y. Zanette. 2018. Fear affects parental care, which predicts juvenile survival and exacerbates the total cost of fear on demography. Ecology 99:127–135.

Easterling, M. R., S. P. Ellner, and P. M. Dixon. 2000. Size-specific sensitivity: applying a new structured population model. Ecology 81:694–708.

Ellner, S. P., and M. Rees. 2006. Integral projection models for species with complex demography. The American Naturalist 167:410–428.

Engen, S., R. Lande, B.-E. Sæther, and M. Festa-Bianchet. 2007. Using reproductive value to estimate key parameters in density-independent age-structured populations. Journal of Theoretical Biology 244:308–317.

Enright, N. J., M. Franco, and J. Silvertown. 1995. Comparing plant life histories using elasticity analysis: the importance of lifespan and the number of life-cycle stages. Oecologia 104:79–84.

Euler, L. 1760. Recherches générales sur la mortalité et sur la multiplicité du genre humain. Mémoires de l'Académie Royale des Sciences et Belles Lettres 16:144–164.

Feng, C. Y., J. P. Ross, D. Mauger, and M. J. Dreslik. 2019. A long-term demographic analysis of spotted turtles (*Clemmys guttata*) in Illinois using matrix models. Diversity 11:226.

Fisher, R. A. 1930. The genetical theory of natural selection. Clarendon Press, Oxford.

Forsythe, A. B., T. Day, and W. A. Nelson. 2021. Demystifying individual heterogeneity. Ecology Letters 24:2282–2297.

Forsythe, A. B., S. P. Otto, W. A. Nelson, and T. Day. 2024. Code and output data associated with Forsythe et al. "Variety is the spice of life: nongenetic variation in life histories influences

population growth and evolvability". Dryad Digital Repository, https://datadryad.org/stash/share/8Yh2oLMu4BXHhrurxgKfd1DEZjM2BqvteGyeyCQ4tz8.

Fox, G. A. 2005. Extinction risk of heterogeneous populations. Ecology 86:1191–1198.

Fox, G. A., B. E. Kendall, J. W. Fitzpatrick, and G. E. Woolfenden. 2006. Consequences of heterogeneity in survival probability in a population of Florida scrub-jays. Journal of Animal Ecology 75:921–927.

Fung, Y. L., K. Newman, R. King, and P. de Valpine. 2022. Building integral projection models with nonindependent vital rates. Ecology and Evolution 12:e8682.

Gillespie, J. H. 1973. Polymorphism in random environments. Theoretical Population Biology 4:193–195.

———. 1974. Natural selection for within-generation variance in offspring number. Genetics 76:601–606.

———. 1977. Natural selection for variances in offspring numbers: a new evolutionary principle. The American Naturalist 111:1010–1014.

Gomes, M. G. M., J. G. King, A. Nunes, N. Colegrave, and A. A. Hoffmann. 2019. The effects of individual nonheritable variation on fitness estimation and coexistence. Ecology and Evolution 9:8995–9004.

González-Suárez, M., J.-F. Le Galliard, and D. Claessen. 2011. Population and life-history consequences of within-cohort individual variation. The American Naturalist 178:525–537.

Gould, A. L., V. Zhang, L. Lamberti, E. W. Jones, B. Obadia, N. Korasidis, A. Gavryushkin, J. M. Carlson, N. Beerenwinkel, and W. B. Ludington. 2018. Microbiome interactions shape host fitness. Proceedings of the National Academy of Sciences of the USA 115:E11951–E11960.

Hamel, S., S. D. Côté, J.-M. Gaillard, and M. Festa-Bianchet. 2009. Individual variation in reproductive costs of reproduction: high-quality females always do better. Journal of Animal Ecology 78:143–151.

Hartemink, N., and H. Caswell. 2018. Variance in animal longevity: contributions of heterogeneity and stochasticity. Population Ecology 60:89–99.

Hernández, C. M., S. van Daalen, H. Caswell, M. G. Neubert, and K. E. Gribble. 2020. A demographic and evolutionary analysis of maternal effect senescence. Proceedings of the National Academy of Sciences of the USA 117:16431–16437.

Hernández-Pacheco, R., and U. K. Steiner. 2017. Drivers of diversification in individual life courses. The American Naturalist 190:E132–E144.

Hooley, D. E. 2000. Collapsed matrices with (almost) the same eigenstuff. The College Mathematics Journal 31:297–299.

Houle, D. 1992. Comparing evolvability and variability of quantitative traits. Genetics 130:195–204.

Huxley, J. 1942. Evolution: the modern synthesis. Allen & Unwin, London.

Jansen, M., P. A. Zuidema, N. P. R. Anten, and M. Martínez-Ramos. 2012. Strong persistent growth differences govern individual performance and population dynamics in a tropical forest understorey palm. Journal of Ecology 100:1224–1232.

Jenouvrier, S., L. Aubry, S. van Daalen, C. Barbraud, H. Weimerskirch, and H. Caswell. 2022. When the going gets tough, the tough get going: effect of extreme climate on an Antarctic seabird's life history. Ecology Letters 25:2120–2131.

Jenouvrier, S., L. M. Aubry, C. Barbraud, H. Weimerskirch, and H. Caswell. 2018. Interacting effects of unobserved heterogeneity and individual stochasticity in the life history of the southern fulmar. Journal of Animal Ecology 87:212–222.

Jenouvrier, S., C. Péron, and H. Weimerskirch. 2015. Extreme climate events and individual heterogeneity shape life-history traits and population dynamics. Ecological Monographs 85:605–624.

Jones, O. R., M. J. Crawley, J. G. Pilkington, and J. M. Pemberton. 2005. Predictors of early survival in Soay sheep: cohort-, maternal- and individual-level variation. Proceedings of the Royal Society B: Biological Sciences 272:2619–2625.

Jouvet, L., A. Rodríguez-Rojas, and U. K. Steiner. 2018. Demographic variability and heterogeneity among individuals within and among clonal bacteria strains. Oikos 127:728–737.

Kendall, B. E., G. A. Fox, M. Fujiwara, and T. M. Nogeire. 2011. Demographic heterogeneity, cohort selection, and population growth. Ecology 92:1985–1993.

Kentie, R., S. M. Clegg, S. Tuljapurkar, J. Gaillard, and T. Coulson. 2020. Life-history strategy varies with the strength of competition in a food-limited ungulate population. Ecology Letters 23:811–820.

Knight, T. M., M. Barfield, and R. D. Holt. 2008. Evolutionary dynamics as a component of stage-structured matrix models: an example using *Trillium grandiflorum*. The American Naturalist 172:375–392.

Krieger, M. S., C. E. Denison, T. L. Anderson, M. A. Nowak, and A. L. Hill. 2020. Population structure across scales facilitates coexistence and spatial heterogeneity of antibiotic-resistant infections. PLOS Computational Biology 16:e1008010.

Lee, A. M., J. M. Reid, and S. R. Beissinger. 2017*a*. Modelling effects of nonbreeders on population growth estimates. Journal of Animal Ecology 86:75–87.

Lee, A. M., B. Sæther, S. S. Markussen, and S. Engen. 2017*b*. Modelling time to population extinction when individual reproduction is autocorrelated. Ecology Letters 20:1385–1394.

Lemaître, J.-F., V. Berger, C. Bonenfant, M. Douhard, M. Gamelon, F. Plard, and J.-M. Gaillard. 2015. Early-late life trade-offs and the evolution of ageing in the wild. Proceedings of the Royal Society B: Biological Sciences 282:20150209.

Leslie, P. H. 1945. On the use of matrices in certain population mathematics. Biometrika 33:183–212.

Lloyd, K. J., W. C. Oosthuizen, R. Fay, M. N. Bester, and P. J. Nico de Bruyn. 2020. Selective disappearance of frail juveniles: consequences for understanding social dominance in adult male elephant seals. Oikos 129:1566–1578.

Mayr, E. 1982. The growth of biological thought: diversity, evolution, and inheritance. Belknap, Cambridge.

Moyes, K., B. Morgan, A. Morris, S. Morris, T. Clutton-Brock, and T. Coulson. 2011. Individual differences in reproductive costs examined using multi-state methods. Journal of Animal Ecology 80:456–465.

Nussey, D. H., T. Coulson, D. Delorme, T. H. Clutton-Brock, J. M. Pemberton, M. Festa-Bianchet, and J.-M. Gaillard. 2011. Patterns of body mass senescence and selective disappearance differ among three species of free-living ungulates. Ecology 92:1936–1947.

Olijnyk, A. M., and W. A. Nelson. 2013. Positive phenotypic correlations among life-history traits remain in the absence of differential resource ingestion. Functional Ecology 27:165–172.

Oosthuizen, W. C., G. Péron, R. Pradel, M. N. Bester, and P. J. Nico de Bruyn. 2021. Positive early-late life-history trait correlations in elephant seals. Ecology 102:e03288.

Orzack, S. H., U. K. Steiner, S. Tuljapurkar, and P. Thompson. 2011. Static and dynamic expression of life history traits in the northern fulmar *Fulmarus glacialis*. Oikos 120:369–380.

Paterson, J. T., J. J. Rotella, W. A. Link, and R. Garrott. 2018. Variation in the vital rates of an Antarctic marine predator: the role of individual heterogeneity. Ecology 99:2385–2396.

Plard, F., C. Bonenfant, D. Delorme, and J.-M. Gaillard. 2012. Modeling reproductive trajectories of roe deer females: fixed or dynamic heterogeneity? Theoretical Population Biology 82:317–328.

Plard, F., J.-M. Gaillard, T. Coulson, and S. Tuljapurkar. 2016. Des différences, pourquoi? Transmission, maintenance and effects of phenotypic variance. Journal of Animal Ecology 85:356–370.

Plard, F., S. Schindler, R. Arlettaz, and M. Schaub. 2018. Sex-specific heterogeneity in fixed morphological traits influences individual fitness in a monogamous bird population. The American Naturalist 191:106–119.

R Core Team. 2023. R: a language and environment for statistical computing. R Foundation for Statistical Computing, Vienna.

Rees, M., and S. P. Ellner. 2019. Why so variable: can genetic variance in flowering thresholds be maintained by fluctuating selection? The American Naturalist 194:E13–E29.

Reznick, D. 1985. Costs of reproduction: an evaluation of the empirical evidence. Oikos 44:257–267.

Rocabert, C., G. Beslon, C. Knibbe, and S. Bernard. 2020. Phenotypic noise and the cost of complexity. Evolution 74:2221–2237.

Ronget, V., M. Garratt, J.-F. Lemaître, and J.-M. Gaillard. 2017. The 'evo-demo' implications of condition-dependent mortality. Trends in Ecology & Evolution 32:909–921.

Rotella, J. J. 2023. Patterns, sources, and consequences of variation in age-specific vital rates: insights from a long-term study of Weddell seals. Journal of Animal Ecology 92:552–567.

Saito, N., S. Ishihara, and K. Kaneko. 2013. Baldwin effect under multipeaked fitness landscapes: phenotypic fluctuation accelerates evolutionary rate. Physical Review E 87:052701.

Salguero-Gómez, R., and J. B. Plotkin. 2010. Matrix dimensions bias demographic inferences: implications for comparative plant demography. The American Naturalist 176:710–722.

Sharpe, F. R., and A. J. Lotka. 1911. A problem in age-distribution. Philosophical Magazine 21:435–438.

Smallegange, I. M., R. E. Fernandes, and J. C. Croll. 2018. Population consequences of individual heterogeneity in life histories: overcompensation in response to harvesting of alternative reproductive tactics. Oikos 127:738–749.

Smiseth, P. T., R. J. S. Ward, and A. J. Moore. 2007. Parents influence asymmetric sibling competition: experimental evidence with partially dependent young. Ecology 88:3174–3182.

Snyder, R. E., and S. P. Ellner. 2018. Pluck or luck: does trait variation or chance drive variation in lifetime reproductive success? The American Naturalist 191:E90–E107.

———. 2022. Snared in an evil time: how age-dependent environmental and demographic variability contribute to variance in lifetime outcomes. The American Naturalist 200:E124–E140.

Snyder, R. E., S. P. Ellner, and G. Hooker. 2021. Time and chance: using age partitioning to understand how luck drives variation in reproductive success. The American Naturalist 197:E110–E128.

Stearns, S. C. 1989. Trade-offs in life-history evolution. Functional Ecology 3:259–268.

Steiner, U. K., and S. Tuljapurkar. 2012. Neutral theory for life histories and individual variability in fitness components. Proceedings of the National Academy of Sciences 109:4684–4689.

Steiner, U. K., S. Tuljapurkar, and T. Coulson. 2014. Generation time, net reproductive rate, and growth in stage-age-structured populations. The American Naturalist 183:771–783.

Steiner, U. K., S. Tuljapurkar, and S. H. Orzack. 2010. Dynamic heterogeneity and life history variability in the kittiwake. Journal of Animal Ecology 79:436–444.

Stover, J. P., B. E. Kendall, and G. A. Fox. 2012. Demographic heterogeneity impacts density-dependent population dynamics. Theoretical Ecology 5:297–309.

Sæther, B.-E., and S. Engen. 2015. The concept of fitness in fluctuating environments. Trends in Ecology & Evolution 30:273–281.

Tompkins, E. M., and D. J. Anderson. 2019. Sex-specific patterns of senescence in Nazca boobies linked to mating system. Journal of Animal Ecology 88:986–1000.

Tuljapurkar, S., U. K. Steiner, and S. H. Orzack. 2009. Dynamic heterogeneity in life histories. Ecology Letters 12:93–106.

Tuljapurkar, S., W. Zuo, T. Coulson, C. Horvitz, and J. Gaillard. 2020. Skewed distributions of lifetime reproductive success: beyond mean and variance. Ecology Letters 23:748–756.

van Daalen, S., and H. Caswell. 2020. Variance as a life history outcome: sensitivity analysis of the contributions of stochasticity and heterogeneity. Ecological Modelling 417:108856.

van de Pol, M., L. W. Bruinzeel, D. Heg, H. P. van der Jeugd, and S. Verhulst. 2006. A silver spoon for a golden future: long-term effects of natal origin on fitness prospects of oystercatchers (*Haematopus ostralegus*). Journal of Animal Ecology 75:616–626.

van Noordwijk, A. J., and G. de Jong. 1986. Acquisition and allocation of resources: their influence on variation in life history tactics. The American Naturalist 128:137–142.

Vattiato, G., M. J. Plank, A. James, and R. N. Binny. 2021. Individual heterogeneity affects the outcome of small mammal pest eradication. Theoretical Ecology 14:219–231.

Vaupel, J. W., K. G. Manton, and E. Stallard. 1979. The impact of heterogeneity in individual frailty on the dynamics of mortality. Demography 16:439–454.

Vaupel, J. W., and A. I. Yashin. 1985. Heterogeneity's ruses: some surprising effects of selection on population dynamics. The American Statistician 39:176–185.

Vindenes, Y., S. Engen, and B.-E. Sæther. 2008. Individual heterogeneity in vital parameters and demographic stochasticity. The American Naturalist 171:455–467.

Vindenes, Y., and Ø. Langangen. 2015. Individual heterogeneity in life histories and eco-evolutionary dynamics. Ecology Letters 18:417–432.

Vindenes, Y., B.-E. Sæther, and S. Engen. 2012. Effects of demographic structure on key properties of stochastic density-independent population dynamics. Theoretical Population Biology 82:253–263.

Zuidema, P. A., R. J. W. Brienen, H. J. During, and B. Güneralp. 2009. Do persistently fast-growing juveniles contribute disproportionately to population growth? A new analysis tool for matrix models and its application to rainforest trees. The American Naturalist 174:709–719.

Figure Legends

Figure 1. Impact of genetic and nongenetic heterogeneity on **A)** mean long-term growth rate (given by the leading eigenvalue, λ_1) and **B)** evolvability (given by the standardized variance in long-term growth rates) across 1000 randomly drawn genotypes when there is early recruitment to the breeding population. The mean long-term growth rate and evolvability (y-axes) are functions of the relative strength of nongenetic variation (x-axes), the sign of the genetic and nongenetic covariance (line colours and panels, respectively), and the type of individual heterogeneity (line types). Note that the average fitness across all genoytpes (i.e., the average number of surviving offspring per parent) is the same in all cases, but the long-term growth rate given by the leading eigenvalue of the corresponding transition matrices rises with positive genetic covariance (blue lines) and, for fixed condition, with positive nongenetic covariance (right panel).

Figure 2. Impact of genetic and nongenetic heterogeneity on **A)** mean long-term growth rate (given by the leading eigenvalue, λ_1) and **B)** evolvability (given by the standardized variance in long-term growth rates) across 1000 randomly drawn genotypes when there is late recruitment to the breeding population. The mean long-term growth rate and evolvability (y-axes) are functions of the relative strength of nongenetic variation (x-axes), the sign of the genetic and nongenetic covariance (line colours and panels, respectively), and the type of individual heterogeneity (line types). Note that the average fitness across all genoytpes (i.e., the average number of surviving offspring per parent) is the same in all cases, but the mean long-term growth rate given by the leading eigenvalue of the corresponding transition matrices rises with the relative strength of nongenetic heterogeneity, unless the vital rates are reset randomly each time step (uncorrelated condition, dashed lines).

Figure 1.

A)

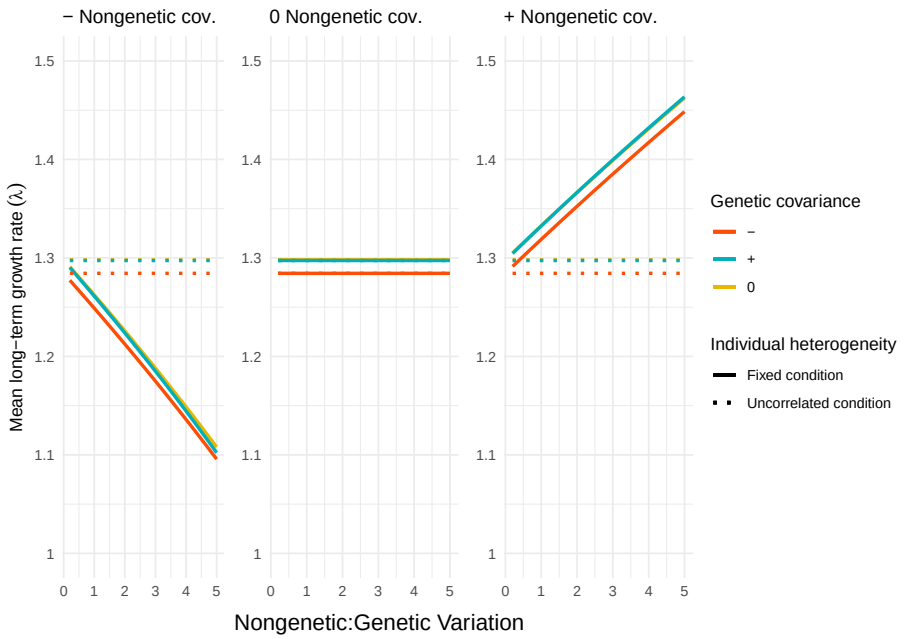
− Nongenetic cov.
0 Nongenetic cov.
+ Nongenetic cov.
Mean long−term growth rate (λ)
1.5
1.4
1.3
1.2
1.1
1
0 1 2 3 4 5
Nongenetic:Genetic Variation
Genetic covariance
−
+
0
Individual heterogeneity
Fixed condition
Uncorrelated condition

B)

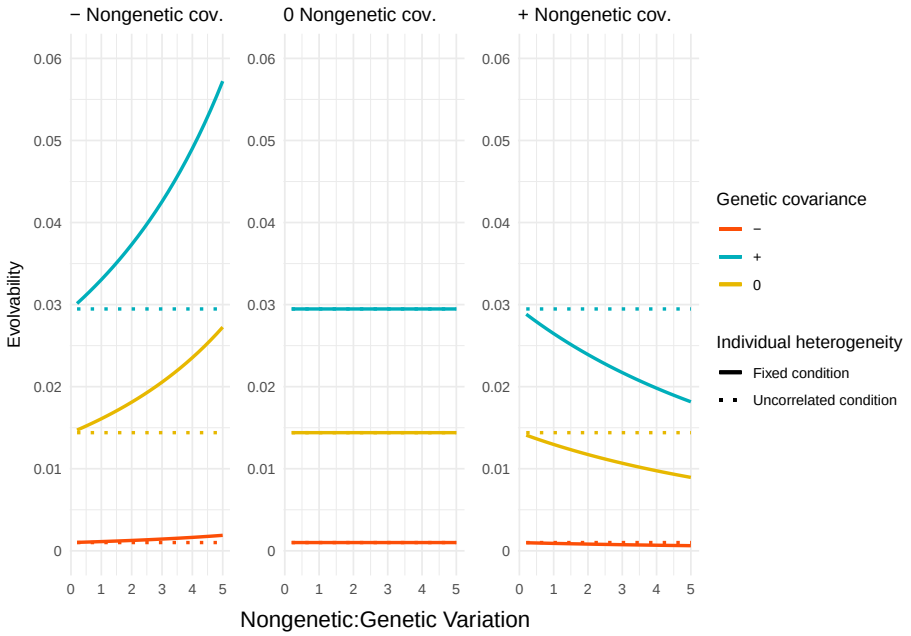
− Nongenetic cov.
0 Nongenetic cov.
+ Nongenetic cov.
Evolvability
0.06
0.05
0.04
0.03
0.02
0.01
0
0 1 2 3 4 5
Nongenetic:Genetic Variation
Genetic covariance
−
+
0
Individual heterogeneity
Fixed condition
Uncorrelated condition

Figure 2.

A)

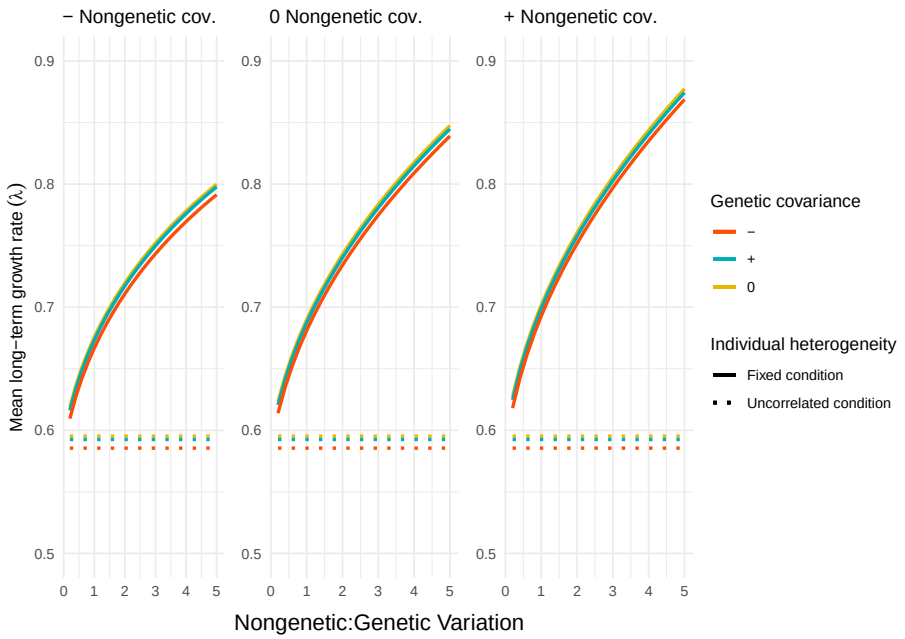
− Nongenetic cov.
0 Nongenetic cov.
+ Nongenetic cov.
Mean long−term growth rate (λ)
0.9
0.8
0.7
0.6
0.5
0 1 2 3 4 5
Nongenetic:Genetic Variation
Genetic covariance
−
+
0
Individual heterogeneity
Fixed condition
Uncorrelated condition

B)

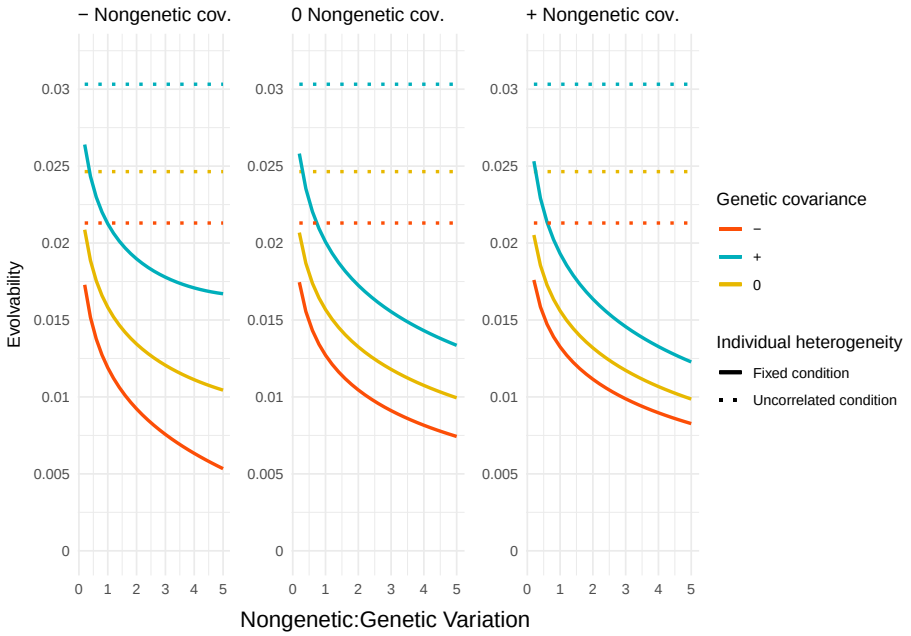
− Nongenetic cov.
0 Nongenetic cov.
+ Nongenetic cov.
Evolvability
0.03
0.025
0.02
0.015
0.01
0.005
0
0 1 2 3 4 5
Nongenetic:Genetic Variation
Genetic covariance
−
+
0
Individual heterogeneity
Fixed condition
Uncorrelated condition